Application of Multispectral Imaging Combined with Data Analytics to Detect Carcass Condemnations during Poultry Processing

By

Micah Telah Black

A thesis submitted to the Graduate Faculty of
Auburn University
in partial fulfillment of the
requirements for the Degree of
Food Science Opt Poultry Science, Master of Science

Auburn, Alabama
May 4, 2024

Rapid detection, poultry, spectral imaging, carcass condemnations, data analytics

Approved by

Dr. Amit Morey, Associate Professor of Poultry Science
Dr. Dianna Bourassa, Associate Professor of Poultry Science
Dr. Moon Kim, Research Leader/Distinguished Senior Research Scientist of USDA-ARS

Abstract

A concern for consumers when buying food is the safety of their food and the risk of foodborne illnesses due to contaminated products. The poultry industry deals with known foodborne pathogens, *Salmonella* spp. and *Campylobacter* spp., that can be found in the gut biome of chicken that are being processed daily. To reduce likelihood contamination of pathogens spreading throughout processing plants, every chicken is visually inspected by USDA-FSIS inspectors or trained processing plant workers when processing whole chicken carcasses. Processing lines move at 140-175 birds per minute making it a difficult to inspect each bird properly for any carcass condemnations such as septicemia-toxemia (sep-tox) and fecal contamination, being a zero tolerance in all food processing plants enforced by USDA-FSIS ruling. With a real-time fluorescent spectral imaging system that can identify carcass condemnations, processing would be easier to target which carcasses will need to be removed for reprocessing or discarded if deemed unacceptable for consumption. With technology advancing daily, improving the inspection system on the processing line is beneficial for plant workers and the safety of consumers' health. After configuring promising camera parameters with two exposure times for fluorescence of photosensitive cells with camera range to explore the advantages of a spectral imaging system, known as the CSI-D+ system, with the detection of sep-tox birds deemed by trained processing workers and fecal contamination on chicken carcasses. Images produced were used for image analysis for classification against carcasses that were condemned. Sep-tox birds were 100% classified correctly against normal carcasses when fluoresced with LED light. Further analysis revealed variations of sep-tox can be identified with an unsupervised image analysis system. Fecal contamination and digesta were identified from the ceca (46%), colon (39%), proventriculus (62%), and small intestine (59.50%) with small and

large applications onto the breast of chicken carcasses with variation of small and large application dots. Additionally, deionized water rinsed fecal contamination carcasses were classified with a 97.80% accuracy against chicken carcasses samples inoculated with *Salmonella* Typhimurium. Rinsed inoculated samples were swabbed and tested with a *Salmonella* PCR assay for further analysis. The presence of *Salmonella* after rinsing was 97.14% for samples that were initially negative before inoculation. These results indicate that spectral imaging can reduce the spread of contamination by decreasing food safety risks at poultry processing plants through providing a resource imaging system for plant workers in comparison to visual inspection.

ACKNOWLEDGMENTS

I would first like to thank God for giving me the knowledge to take on this task in life. I would like to acknowledge and extend my gratitude to my committee members for their guidance and support throughout my master's program. Dr. Amit Morey, a great mentor and professor, has taught me numerous lessons throughout my professional and academic journey over the years. His grace and persistent encouragement to keep working towards my goals in life will always be something I will reflect upon throughout my life. Dr. Moon Kim has been inspirational aspect in this chapter of my life. He has been supportive and provided guidance into my process from the beginning. Dr. Bourassa, I thank you, for your guidance and inspiration to look at things beyond the surface. She has been very helpful in preparing my thesis for publication and a great encourager. Dr. Laura Garner, I would like to acknowledge and thank for being supportive throughout the years with advice and different perspectives and a person to lean on during the ups and downs of life.

Others who have graduated before me have been inspiration and instrumental in helping complete this research. I am grateful for my colleague, Dr. Aftab Siddique, for assisting in the analytical processes of this data. This was a collaborative research with Safety Spect, Inc. team and the USDA-ARS team located in Beltsville, MD for funding and resources. Thank you for your guidance and experiences shared with me.

I need to thank my family and friends for their support and encouragement given throughout these years. My mom and dad, Leonard and. Vonita Black, for providing constant unconditional love, support, and advice in my academic years. My brothers, sisters, and God family for the continued checking in and support shown over these years. I dedicate this thesis to Vonita Black, as one of my last promises I gave her, was to see this all the way through.

Table of Contents

Abstract……ii

Acknowledgments……..iv

List of Tables……vii

List of Figures……...viii

Chapter I. Literature Review……1

Introduction……..2

Background on Sep-tox and Foodborne Pathogens Common in the Poultry Industry……4

The Problems and Complications of Processing Plants……...6

Background on Rapid Detection……..9

Spectral Imaging……16

Data Analytics……24

Conclusion……29

References……..30

Chapter II. Identification and Classification Broiler Carcasses Exhibiting Septicemia-Toxemia using Spectral Imaging Systems……35

Abstract……..36

Introduction……37

Materials and Methods……...40

Experimental Design……..40

Multispectral Imaging System……...42

Image Classification……..43

Results and Discussion……..47

Conclusion…….55

References……..57

Chapter III. Application of Fluorescence Imaging on Chicken Carcasses for the Detection of Visible and Invisible Fecal Contaminations……..59

Abstract……..60

Introduction……61

Materials and Methods……...64

Multispectral Imaging System……...64

Detection of fecal matter from four regions of the GI tract……...65

Detection of fecal contamination invisible to the naked eye and occurrence of *Salmonella*……..66

In-plant validation of the CSI-D+ and presence of *Salmonella*……67

PCR Assay……67

Image Classification……..68

Results and Discussion……..69

Fluorescence Imaging……....69

Classification model performance for different contaminants……..73

Classification model performance for invisible contamination……76

Salmonella PCR assay……...77

Conclusion…….78

References…….80

Chapter IV. Summary……82

List of Tables

Table 1.1. Different rapid techniques used in poultry matrices to detect bacteria……9

Table 1.2. The advantages and disadvantages of rapid detection techniques……15

Table 2.1. Summary of sessions displaying the number of carcasses and carcass images taken with camera parameters listed in Table 2.2……42

Table 2.2. CSI-D+ camera parameters utilized for all sessions, where the settings for sessions 1-4 are recognized as A, and the reframed parameters in sessions 5-12 are recognized as B…...47

Table 2.3. Microsoft Custom Vision classification accuracies of sep-tox and normal images at 50% and 85% thresholds displaying performance percentages per class for precision, recall, and accuracy percentage……50

Table 3.1. Settings used for CSI-D+ imaging system to fluoresce in ambient light-free conditions..……65

Table 3.2. Summation of percentage accuracy average and standard deviation for classification between fecal contaminants exposure time and contaminant size from CNN model performed in Google Collaboration.……75

Table 3.3. Individual percentage accuracy for classification of fecal matter contaminants sizes and exposure times from Azure Custom Vision displaying accuracy percentage (AP) with threshold.……75

Table 3.4. Overall percentage accuracy for classification of fecal matter contaminants sizes and exposure times from Azure Custom Vision displaying precision, recall, and accuracy percentage (AP) with threshold.……...75

Table 3.5. Percentage accuracy for classification of fecal contamination exposure times before inoculation, during inoculation, and rinsed samples from Azure Custom Vision displaying precision, recall, and accuracy percentage (AP) at two thresholds.……...76

Table 3.6. Percentage accuracy of overall images before inoculation, during inoculation, and rinsed samples from Azure Custom Vision displaying precision, recall, and accuracy percentage (AP) at two thresholds.……...……..77

Table 3.7. Swabbed samples from before inoculation, during inoculation, and after rinsing of fecal contamination for the presence or absence of *Salmonella* spp. using GeneUp® PCR machine.……78

Table 3.8. Plant setting swabbed samples from contaminated and after rinsing of fecal contamination for the presence or absence of *Salmonella* spp. using GeneUp® PCR machine.……78

List of Figures

Figure 2.1. Experimental design of camera set up to remove ambient light.……42

Figure 2.2. Spectral images of sep-tox and normal carcasses taken at exposure times of 175 ms (a-b) and 350 ms (c-d) at initial setting A used for sessions 1-4, showing oversaturation.……...48

Figure 2.3. Spectral images of sep-tox and normal carcasses taken at exposure times of 230 ms (a-b) and 270 ms (c-d) with updated camera parameters B, sessions 5-12, for grey-scale imaging..……49

Figure 2.4. Heatmap for overall classification of sep-tox and normal carcass images from sessions 5-12.…….49

Figure 2.5. Bar graph of sep-tox bird images……52

Figure 2.6. Scatterplot of sep-tox bird images.……..52

Figure 2.7. Sep-tox images from Cluster 1 (a), Cluster 2 (b), and Cluster 3 (c) displaying the differences observed in each cluster.…….53

Figure 3.1. Images of chicken carcass at with fecal matter of (a-b) ceca, (c-d) large intestine, (e-f) proventriculus, and (g-h) small intestine with both small and large applications of rubber stamp at 230ms exposure……..71

Figure 3.2. Images of chicken carcass at with fecal matter of (a-b) ceca, (c-d) large intestine, (e-f) proventriculus, and (g-h) small intestine with both small and large applications of rubber stamp at 270ms exposure.…….72

Figure 3.3. Images of chicken carcass before inoculation of fecal matter, with inoculation of fecal matter, and after rinsed with deionized water at exposure times of (a-c) 230ms and (d-f) 270ms.……73

Chapter I.

Literature Review

INTRODUCTION

Consumers' main concerns when buying poultry products is the safety of their food and food diseases that are caused by bacterial contamination (Super, 2018). Bacterial contamination can develop from fecal contamination through improper feed withdrawal, the piling of birds during rehanging in a processing plant, or from processing issues involving the scalder and picker. The main pathogens present in the poultry industry are *Salmonella* spp., *Campylobacter* spp., and *Listeria monocytogenes*. These foodborne pathogens can cause serious bacterial infections that are sometimes fatal to humans and animals. *Salmonella* and *Campylobacter* are known foodborne pathogens found in poultry processing plants. Every year these bacteria cause millions of infections, meanwhile *L. monocytogenes* can take a more lethal approach, giving this pathogen one of the highest mortality rates amongst food borne pathogens if ingested (CDC, 2021b). These bacteria are important to food safety and quantifying them within the industry can be done by running tests such as the most probable number (MPN) on samples that have the possibility of being contaminated. Methods such as USDA-FSIS MLG 4.14 method for *Salmonella*, 8.14 method for *Listeria monocytogenes*, and 41.07 method for *Campylobacter jejuni/coli/lari* can take up to four to seven days for confirmation for each bacterium to their respective tests (USDA-FSIS, 2023). With rapid techniques such as multispectral imaging and real time PCR assay, test results can be given within a few minutes to hours reducing the amount of time it would take to do Most Probable Number (MPN) method, a traditional culture method. Rapid detection has made a significant change to detect bacterial problems throughout processing and further processing plants allowing production agencies to determine a faster decision in disposition.

The United States Department of Agriculture Food Safety and Inspection Service (USDA-FSIS) has an important job in ensuring the safety of food for consumers given the United States is the largest broiler producing country (NCC, 2022). With poultry carcass condemnations and foodborne diseases being spectated within the processing plant, having sufficient food safety approaches for post-slaughter inspection are imperative in case reprocessing has to occur. In conventional poultry processing systems, inspection is overseen by FSIS workers, along with plant workers, that are placed along the processing line near the evisceration station inspecting each chicken carcass that is processed. The inspection transpired is by visual and physical inspection of both the carcass and the viscera that have been extracted (Chao, 2010). A new system was introduced in 2014 by the FSIS where the poultry processing plants could voluntarily implement a program named the 'New Poultry Inspection Service' (NPIS) (USDA-FSIS, 2014). The NPIS program allowed trained processing workers to oversee the inspection of the chicken being processed for any unwholesome carcasses presented on-line before FSIS inspectors receive them at their stations (USDA-FSIS, 2014b). With the inspectors allowed to focus on more food safety related issues, this system allows microbial testing and to be more attended to on processing lines from the FSIS inspectors. Some of the carcass condemnations being examined and removed from the processing line are air sacculitis, ascites, bruises, cadavers, dead on arrival, fecal contamination, inflammatory issues, synovitis, and tumors (USDA-FSIS, 2014). These inspections can lead to false identifications of a condemned carcass or normal carcass due to the speculation of the naked human eye when the speed of the processing line is moving as fast as 140-175 birds per minute (bpm). Visual inspection can become more difficult with the increased demand of chicken in the industry due to an influx of carcasses that would be overseen making difficult to be thoroughly examined. Fecal

contamination on chicken carcasses from the ceca, large intestine (colon), small intestine and ingesta, from the proventriculus or crop, can be found on chicken carcasses as well during inspection which is a “zero-tolerance” policy according to USDA-FSIS regulations specified in their HACCP model (USDA-FSIS, 2014a). With the line speed rapidly moving, small amounts of fecal contamination could be overlooked in these conditions by the naked eye of the plant workers and FSIS inspectors and enter the processing system contaminating other birds and processing equipment. Contamination would be detrimental as over 9 billion chickens are produced yearly for consumers in America. With the mass consumption of poultry products, processing plants will need a more beneficial inspection system overtime.

Background On Sep-Tox and Foodborne Pathogens Common in The Poultry Industry

Septicemia-toxemia in Chicken. Septicemia-toxemia is one of the most common carcass condemnations found in the poultry industry (USDA-NASS, 2024). Septicemia-toxemia, also known as sep-tox, is a bacterial infection that causes systemic changes within the bird. Sep-tox can be identified by visual petechial hemorrhages on the following: heart, liver, kidneys, muscles, and membranes. Another identification is the red appearance to their skin, the underdevelopment in size of the bird, and inflammation to the spleen, liver, and kidneys. Once a bird is deemed as sep-tox, it is to be removed from the processing line and named condemned. There are multiple bacteria that can cause sep-tox in chicken. Depending on the severity of the bacterial infection, the chicken can have a full recovery or can lead to fatality. A significant identification of sep-tox is through the redness of the skin on these diseased birds. This redness of the skin can vary from a pale white to a purple-reddish color to the skin depending on the level of bacterial infection is found within the bloodstream of the chicken.

Salmonella spp. One of the most common bacteria found during poultry processing that infect and cause outbreaks in people is *Salmonella* spp. In 2011, these bacteria were the top leading causes of foodborne illnesses in the United States (Scallan et al., 2011). *Salmonella,* from the family Enterobacteriaceae, is a gram-negative bacterium with over 2,000 serotypes was discovered by Dr. Daniel Salmon in 1885 (CDC, 2021a). Its physical attributes are rod shaped with flagella for motility. The chemical makeup of this gram-negative food borne pathogen contains H and O antigens. These antigens help the different serotypes be distinguishable between one another. The O antigen is the outermost portion of the cell wall surface, while the H antigen is the slender-like structure also known as the flagella (CDC, 2021a). This bacterium is non-spore forming and attacks the gastrointestinal tract.

Salmonellosis is an infectious bacterial disease that is caused by a small percentage of the known serotypes. This occurs when the foodborne pathogen itself is ingested and adaption to the gastrointestinal tract is sustained where it will remain and multiply. Symptoms start developing around twelve to seventy-two hours after contracted into the body (Center for Food Safety and Applied Nutrition, 2019). This bacterial infection typically lasts four to seven days and can be survived without treatment by most. *Salmonella* can be split into two species, *S. bongori* and *S. enterica,* where more than 2,000 serovars exist. *Salmonella enterica* subspecies *enterica* contains all of the human pathogenic types. *Salmonella bongori* and *S. enterica* can be separated into three groups: human infected only, host-adapted serovars, and unadapted serovars. The human infected only group includes typhoidal and paratyphoidal species. This group has a long incubation time while having a high mortality rate. Examples of typhoidal serotypes, *S. typhi* and *S. paratyphi,* cause typhoid fever and paratyphoid fever, also known as enteric fever. These serotypes can only be found in humans and can be passed along from one human to the next.

Typhoidal *Salmonella* can enter into the bloodstream and create more alarming problems by getting into other organs throughout the body or causing septic shock causing hospitalization known as typhoid fever. The host-adapted group are species of *Salmonella* where some are human foodborne pathogens. Some examples of host-adapted pathogens are *S. Gallinarum, S. Dublin, and S. Abortusovis*. The final group is the unadapted serovars which are also known as non-typhoidal. The non-typhoidal serotypes of *Salmonella* are known for infecting humans and animals that can only be found in the gastrointestinal tract (Bharmoria et al., 2017). When infected with salmonellosis, common symptoms experienced will be the following: diarrhea, fever, and abdominal cramps (Center for Food Safety and Applied Nutrition, 2019). If experiencing a harsher case of this illness, symptoms can develop into body aches, lethargy, blood present in the urine or feces, and can also result in death (Center for Food Safety and Applied Nutrition, 2019). *Salmonella* is dangerous to contract, and the most common way to contract salmonellosis is through animal feces that either seeps through soil or is displaced on edible parts of the animal. Some strains of *Salmonella* have become resistant to antibiotics making it very difficult to rid of the illness if caught. *Salmonella* strains that are most associated with poultry and human food supply are *S.* Enteritidis, *S.* Typhimurium, and *S.* Heidelberg (Robinson, 2018). *Salmonella* Enteritidis is the most common strain that is present in poultry and food supply infecting the gastrointestinal tract of the chicken (Robinson, 2018). *Salmonella* is spread habitually through fecal matter.

The Problems and Complications of Processing Plants

The poultry industry battles bacterial contamination with *Salmonella spp.* and *Campylobacter spp.* in the processing plant as these microorganisms are commonly found in the poultry birds' gut biome. These bacteria are most commonly found in the fecal matter of the

birds and can become displaced on the feathers and feet of the birds due to improper feed withdrawal. Having proper feed withdrawal indicates no access to food between 8-12 hours before slaughter. If farmers, poultry processors, and/or third parties do not adhere to the feed withdrawal timeline, the exposure to fecal contamination increases because of the degradation of the intestinal walls at 13 hours. Respecting the allotted time for feed withdrawal decreases chances of fecal contamination given the excrement of feces will decrease because there will be little to nothing in the crop, proventriculus, or ventriculus (gizzard). Additionally, with the proper feed withdrawal, the small intestine and large intestine have minimal ingesta located in these organs.

Rapid resolutions on problems.

According to the Food Safety and Inspection Service (FSIS), they require a "zero tolerance" policy for fecal material that can be visibly seen with the naked eye at the time of inspection (USDA-FSIS, 2019). Even with this policy, there are still outbreaks of *Salmonella* and *Campylobacter* in the poultry industry. *Listeria monocytogenes* is found more frequently in further processing plants but have the possibility of being in raw chicken meat causing problems in the processing plants and has a "zero tolerance" policy in RTE meat and poultry products (Gallagher et al., 2003). To help reduce the number of outbreaks from these bacteria, rapid detection will help save time and money overall by performing detection methods in real-time than performing standard tests lowering food safety risk. Currently to test for food borne pathogens in food, some process plants have their samples sent off to a laboratory and analyzed (Romero & Cook, 2018). Enumerated tests can take over a course of four to seven days to get a confirmation of the bacteria present in the environment or samples that may be given to test

according to the USDA. Standard methods also include extensive training and continual purchases of expensive reagent kits and media (Joo et al., 2012). Although the standard methods are reliable for results, however it is not able to give real-time information on the absence or presence on the bacteria (Romero & Cook, 2018). Rapid detection is a newer and better choice of testing to detect bacterial issues to implement proactive methods in hopes to reduce the millions of cases of infections that these bacteria spread. Rapid detection can consist of techniques using swabbing to hyperspectral imaging.

Table 1.1. Different rapid techniques used in poultry matrices to detect bacteria

Method	*Date*	*Matrix*	*Organism*	*Duration*	*Author*	*Did it work?*
Multiplex PCR method	1994	Raw and cooked chicken products	*Listeria monocytogenes*	1h	Lawrence & Gilmour, 1994	Yes
Single-pipetting microfluidic assay	2013	Poultry packaging	*Salmonella*	30 seconds	Fronczek et al., 2013	Yes
Dot blot and PCR	2014	Poultry skin from wing and thigh	*Campylobacter*	1-2 days	Fontanot et al., 2014	Yes
Rapid Colorimetric Immunoassay	2015, 2018	Chicken liver; Chicken meat, glass slide, and stainless-steel surfaces	*Salmonella*, *Campylobacter*	50-60 minutes	Alamer et al., 2018; Sun et al., 2015	Yes
Rapid LAMP-based method[3]	2017; 2018	Chicken breast; Raw chicken meat	*Campylobacter*, *Listeria monocytogenes*	1h	Romero and Cook, 2018; Wachiralurpan et al., 2017	Yes
HSI[2]	2019	Glass slides	*Salmonella*, *Campylobacter*, *Listeria monocytogenes*	5-15 minutes	Michael et al., 2019	Yes
SPIA[4]	2020	Various part of raw chicken samples	*Salmonella*	1h	Yang et al., 2020	Yes
HMI[1]	2021	Broiler chicken carcass rinses	*Campylobacter*, *Listeria monocytogenes*, *Salmonella*	1h	Eady & Park, 2021	Yes

[1]HMI = hyperspectral microscope imaging
[2]HSI = hyperspectral imaging
[3]LAMP = loop-mediated isothermal DNA amplification
[4]SPIA = single primer isothermal amplification

Rapid colorimetric immunoassay using cotton swabs and nanobeads

Principle. Immunoassay uses antigens (proteins) and antibodies bound together to help identify and measure certain substances (Health, 2021). Control groups are cultured onto media and used to prepare for the experiment (Alamer et al., 2018; Sun et al., 2015). Colorimetric immunoassay is used for on-siter detection (Alamer et al., 2018; Sun et al., 2015). This technique uses nanoparticles that have been modified with antibodies of the pathogenic bacteria in order to produce the fluorescence color when the bacteria is present (Alamer et al., 2018; Sun et al., 2015). Magnetic separation and buffer rinsing are used on the samples to remove any nanoparticles not attached (Alamer et al., 2018; Sun et al., 2015). Once rinsing and magnetic separation has been performed, the nanoparticles will illuminate and show the presence or absence of the bacteria (Alamer et al., 2018; Sun et al., 2015). Quantitative results are able to be determined depending on the brightness or dullness of the nanoparticles (Alamer et al., 2018; Sun et al., 2015).

Technique. In this experiment, Alamer et al. (2018) worked with rapid colorimetric immunoassay to detect bacteria *Campylobacter* and *Salmonella* on solid surfaces and chicken breast. A good recovery of pathogens results in swabbing plastic, stainless steel, and wood surfaces with a cotton swab and placing in an extraction buffer later (Alamer et al., 2018). The extracted buffer is placed into an applied technique (e.g., colored nanobeads) or plated after it is vortexed. Alamer et al. (2018) were looking for a method that could be cost-efficient and handy while also producing results in a timely manner. This cotton swab method was contrived with immunoassay proposal that has specific antibodies that detects each bacterium (Alamer et al., 2018). The swabs were able to detect pathogens: *Salmonella typhimurium, S. Enteritidis, and Campylobacter jejuni* from surfaces located in processing plants (Alamer et al., 2018). Sun used

Salmonella pullorum as its target bacteria, along with four other bacteria, in the experiment (Sun et al., 2015). The buffer that the cotton swab is placed into will differentiate the bacteria with colored nanobeads that are specific to the related bacteria (Alamer et al., 2018). In the experiment Sun orchestrated, magnetic particles and blue-silica nanoparticles were modified with antibodies to create antibody-coated magnetic and silica nanoparticles to help with identification (Sun et al., 2015). Alamer et al. (2018) and Sun et al. (2015) used the sandwich immunoassay to help enable the detection of bacteria from a solid surface by using a single device in a centrifuge tube. A DNA extraction kit and real-time PCR were needed in helping with this experiment (Alamer et al., 2018). While Alamer used PCR to help assist with his project, Sun (2015) used a scanning electron microscope to read the wavelengths of the bacteria (Sun et al., 2015). The *Salmonella* strains were grown in trypticase soy broth after being in 20% glycerol solution that was stored in -80 ^{o}C (Alamer et al., 2018). After eighteen to twenty hours of incubation at 37 ^{o}C, they were centrifuged at 10000 Xg for ten minutes at 4 ^{o}C and washed in TSB broth twice (Alamer et al., 2018). Cell suspensions were primed and adjusted to 10^8 cfu/mL and immediately diluted serially in TSB broth to 10^8 cfu/mL (Alamer et al., 2018). *Campylobacter jejuni* stayed in a 37 ^{o}C incubator for four hours and moved to microaerophilic conditions enriched in Bolton broth for 24-28 hours while incubated at 42 ^{o}C and made into ten serial dilutions (Alamer et al., 2018). Alamer et al. (2018) were able to activate the cotton swabs by submersing them in solution that contained 100 mL of 2mM sodium periodate ($NaIO_4$) and 1 mL of sulfuric acid overnight at room temperature and washed in cold distilled water to remove any excess oxidizing agent (Alamer et al., 2018). Activated aldehyde group that is found in the cotton swab is used to help identify the antibodies by their amino groups (Alamer et al., 2018). Sun grew bacteria in lysogeny broth at 37 ^{o}C (Sun et al., 2015). Alamer (2018) used 300

microliters (µl) of magnetic or polymer beads in different colors to represent the different types of pathogens. 100 µl of blue nanoparticles were used to help identify *S. pullorum* (Sun et al., 2015). To bind the beads with the antibodies, Alamer (2018) incubated the two together overnight. For the screening technique, there is two steps wherein the first step the beads are now antibody-linked and prepared to be conjugated with the cotton swabs to develop the color solution from the nanobeads for the secondary antibody detection (Alamer et al., 2018). Chicken, glass, and stainless-steel surfaces were contaminated in a 20x20 cm square by the pathogens and swabbed for confirmation after 10 minutes (Alamer et al., 2018). The second step involves the detection of the bacteria sandwiched in between the cotton swab and the colored nanobeads that were rinsed in a buffer for two minutes (Alamer et al., 2018). Whichever specific-colored beads trapped on the cotton swab indicated which pathogen was detected by the stained cotton swab on the contaminated surfaces (Alamer et al., 2018). PCR was used to confirm for DNA matches to the bacterial cultures following the protocol given by QIAGEN running for approximately forty minutes (Alamer et al., 2018; Robert-Rössle-Strasse, 2021). The results displayed that as the more enumeration of the bacteria was present, the more intense the colors were on the cotton swab limiting the number of pathogenic bacteria can be found on surfaces (Alamer et al., 2018). Sun et al. (2015), however did not use cotton swabs for identification but a microplate reader to identify the bacteria that were bound to magnetic nanoparticles. An increase of absorbance at 675 nm and an apparent blue color were identified when it came to *S. pullorum* being present. Sun et al. (2015) noticed that that an increase in recovery of more nanoparticles occurred with longer incubation periods at thirty minutes. A difference between Alamer et al. (2018) and Sun et al. (2015) experiments were that stability of the nanoparticles were performed over a course of 1, 7, 30, 60, and 90 days in Sun's experiment. These nanoparticles were left in storage at 4 ^{o}C and

remained stable showing that anti-*S. pullorum* molecules on the surface are maintaining immobility (Sun et al., 2015).

Hyperspectral microscope imaging (HMI)

Principle. This technique collects microscopic data in a three-dimensional (3D) hypercube matrix with two dimensions, spatial and spectral (Anderson et al., 2008). The two dimensions represent spatial data (x and y coordinates), and another represent spectral data (λ) to help identify the unique photosensitive properties of bacteria (Eady et al., 2015). A typical colony is picked from an agar plate and inoculated into 100 µl of deionized water, vortexed, and placed to dry onto a glass microscope slide (Eady & Park, 2021). The microslide is covered with a coverslip and placed on the sample stage of the hyperspectral microscope imaging and surveyed (Eady & Park, 2021). Microslides are read with a tungsten halogen (TH) light with a wavelength peak of 630 nm (Eady & Park, 2021). Images are captured and shown by cell segmentation by highlighting the outside of the cells in a black and white contrast (Eady & Park, 2021).

Technique. In a previous study, Anderson et al. (2008) was able to differentiate between living and dead damaged *Bacillus anthraces* spores through HMI technique. Eady and Park (2015) performed an experiment using a hyperspectral microscope imaging system with *Salmonella* that allowed them to see different serotypes of the bacteria species. An approach known as discriminant analysis (DA) was performed in eight hours or less resulting in a single-cell based mean pixel intensity pattern for imaging (Eady et al., 2015; Eady & Park, 2021). Eady and Park (2021) wanted to continue improving the opportunities of HMI and honed on expanding the classification verification this technique's ability possesses. Since the previous experiment gave a pixelated image, they constructed a soft independent model of class analogy

(SIMCA) approach to get a "yes/no" answer when in the presence of *Salmonella* (Eady & Park, 2021). SIMCA was a better approach than DA in this experiment for the reasons of rejecting a sample if the product was outside of the model's calibration boundaries avoiding any false negatives (Eady & Park, 2021). In Anderson et al. (2008) project, a goal was to see the viable spores after being introduced to chlorine and hydrogen peroxide mixtures while requiring hyperspectral reflectance reference signatures in those cultures. Eady et al. (2015) wanted to examine spectral signatures of bacteria grown at 24-hour culture compared to cultures that were grown at 6, 8, 10, and 12-hour cultures as their first objective. The second objective was identifying and differentiating five serotypes of *Salmonella* through spectral signatures at their cellular level (Eady et al., 2015). The most previous study that involved Eady and Park (2021) wanted to accurately predict presence of *Salmonella* that can be compared to PCR and enriched plating with a 95% accuracy rate. To start off the experiment for Eady and Park (2021), carcass rinses were performed on broiler chicken finding a multitude of bacteria that included *L. monocytogenes*, fourteen species of *Salmonella*, and a few others. Additionally, three species of *Campylobacter* stock cultures that were used in this project, but not found in the carcass rinses, were grown on agar media at the respective time and temperature (Eady & Park, 2021). After the cultures were harvested from incubation, sample slides for each species were made and stored in 4 ^{o}C until HMI was ran within the next day (Eady & Park, 2021).

ADVANTAGES/DISADVANTAGES

Table 1.2. The advantages and disadvantages of rapid detection techniques.

Type	Advantages	Disadvantages
Dot blot and PCR	• Able to identify different DNA sequences of *Campylobacter* (Fontanot et al., 2014)	• 24h enrichment is required for PCR testing (Fontanot et al., 2014) • Did not see positive results at 0,6,12 h (Fontanot et al., 2014)
HMI	• Reduces false negatives from occurring (Eady & Park, 2021) • Able to distinguish between *Salmonella* serotypes (Eady & Park, 2021)	• Selectivity increase can be improved (Eady & Park, 2021)
MSI	• Salmonella strains were able to be distinguished between another (Michael et al., 2019) • Can be performed in 15 minutes while producing images in 5 minutes (Michael et al., 2019) •	• Expensive (Michael et al., 2019) • Cross-validation only worked for some bacteria with a specific genus (Michael et al., 2019)
Multiplex PCR method	• Can be done within an hour (Lawrence & Gilmour, 1994) • Can differentiate between *Listeria* spp. and *L. monocytogenes* (Lawrence & Gilmour, 1994)	• Older method (Lawrence & Gilmour, 1994)
Rapid colorimetric immunoassay	• Cost-efficient and easy to use, simple (Alamer et al., 2018) • Can be spotted with the bare eye (Alamer et al., 2018) • Instrument-free (Alamer et al., 2018)	• Preparation for cotton swabs takes up to 2 days of preparation for use (Alamer et al., 2018; Sun et al., 2015) • Detection limit (Alamer et al., 2018) • Semi-quantitative (Alamer et al., 2018)
Rapid LAMP-based method	• Takes an hour to achieve results (Romero & Cook, 2018)	• Ran into false negatives if samples were < 800 cfu/swab when detecting *Campylobacter* (Romero & Cook, 2018)
SPIA	• Specific amplification (Yang et al., 2020) • Can be seen with visual fluorescence by day light (Yang et al., 2020)	• Cannot differentiate between dead and living cells (Yang et al., 2020)
Single-pipetting microfluidic assay	• Results in less than a minute and easy to use (Fronczek et al., 2013) • Can maintain a good condition in storage up to 8 weeks (Fronczek et al., 2013)	• Has a dip in enumeration around the two-well chip at 10^2 -10^3 cfu mL^{-1} (Fronczek et al., 2013)

cfu= colony forming units
HMI= hyperspectral microscope imaging
MSI= multispectral imaging
SPIA = single primer isothermal amplification

SPECTRAL IMAGING

Spectrography is an emerging spectral technology allowing numerous (more than three to hundreds) spectral bands to be observed throughout the electromagnetic spectrum simultaneously combining spectroscopy and imaging into one (Qin et al., 2011; Michael et al., 2019). MSI is another technology that allows rapid detection of bacteria to occur and has been used in multiple fields like agriculture and medicine (Eady et al., 2019). Multispectral (MSI) imaging displays the fluorescence of the substance being examined at hand through the visible light wavelength spectrum. MSI uses a range of 200-1000 nm on the visible near-infrared spectra by reflecting light back to the camera in order to receive a seen figure (Michael et al., 2019; Sueker et al., 2021). This technology allows foodborne pathogenic bacteria or contaminants to be detected at a faster rate than the standard method taking four to seven days for results by reducing the time down to fifteen minutes relieving the laborious workload of traditional methods at a presumptive level of traceable pathogens (Michael et al., 2019). Spectral imaging is a means to additionally help identify contamination on surfaces and on food products. Through the fluorescence sensing techniques, quality assessments on foods were applied when using spectral imaging for being a great source in food sciences such as meat samples for characteristic measures (Kim et al., 2006; Sueker et al., 2021). Spectral imaging has been used to help depict fluorescence properties of chicken carcasses that showed condemnations and diseases compared to a wholesome bird examining the skin of the breast (Kim et al., 2006). This rapid detection method is used to help with detection of inorganic materials present on the surfaces of vegetables, meats, fruits, and diverse processed foods for quality purposes (Peng and Dhakal, 2015; Chao et al., 2020). Fluorescence production through spectral systems has been a useful tool for inspection to assist with food safety with specific spectra for biological residues in visible and near-infrared wavelengths (Sueker et al., 2021). Meat

products and proteins have shown illumination in UV, blue, and green wavelengths while fecal matter from dairy cows emit red illumination that peak at 680 nm when UV radiation was excited at 360 nm (Wold et al., 1999; Kim et al., 2003; Sueker et al., 2021).

Principle. This technique utilizes three to hundreds of wavelengths that is measured in nanometers (nm) to help display an image that can also use ultraviolet (UV) light to fluoresce what may be present on the surface of objects. Spectral imaging uses wavelengths that typically spans from 400 to 700 nm known as visible light, to help with accurate color representation. Some spectral systems use infrared or UV light, where wavelengths range from 700 to 1,000 nm for infrared and 100 to 400 nm for UV. There are three types of UV light used and are the following: UV-A, UV-B, and UV-C. UV-A (315-400 nm) and UV-B (285-315 nm) lights are used for fluorescent of organic materials while UV-C (100-285 nm) is a stronger, more dangerous light used for disinfection of bacteria, fungi, and viruses on surfaces. UV-C can be commercially made for disinfection but naturally, it will rarely reach the skin's surface due to the length of its wavelength. Spectral imaging is used to rapidly detect and provide documentation of visible and invisible organic materials and pathogenic biofilms (Sueker et al., 2021). Ultraviolet light has been used for in the food industry previously for sanitation purposes and is finding its way into food distributing companies and processing plants for preventative purposes with contamination inspection to help with the avoidance of recalls and the spread of bacterial exposure to the consumers. Spectroscopy is used to help develop a more automized system for food processing plants with inspection of products going to consumers in search to reduce outbreaks of foodborne pathogens and maintaining distribution of high-quality foods. Although spectroscopy uses a range of wavelengths, each imaging system has different wavelength ranges that are used to fit each specific environment.

Technique. Research involving spectral imaging has constantly been developed since the 1990s, specifically on chicken meat for detection of wholesome versus unwholesome birds. USDA-ARS scientists, Chen and Massie (1993) used visible and near-infrared reflectance spectroscopy systems to distinguish chicken carcasses that are identified as cadavers, septicemic, and normal birds for veterinarians. Wavelength parameters ranging from 500 to 1113 nm were used in a completely dark room on cold (0º C) and warm (20º C) carcasses with a diode array detector with an average 200 scans per spectrum using over 250 chicken carcasses in total (Chen and Massie, 1993). Classification was formed with a training and test set by separating the odd and even numbered cases out, further allowing model systems to be made depending on the characteristics shown through the reflectance and interactance in the training sets where the temperature was not a factor in these sets. To evaluate these class functions, a multiple linear regression was performed to help classify normal and septicemic birds, but cadavers were not a part of this first regression. A second regression was made where the septicemic birds were not used but the normal and cadaver carcasses were used for classifier functions. A third regression was made to form classifier functions for the unwholesome carcasses. After classifiers were created, wavelengths showing variation between the samples were selected resulting in four wavelengths variations. As a result, there was distinct separation in the training set for reflectance spectra for the normal carcasses when compared to the septicemic and cadaver carcasses at several wavelength absorption bands that were under 850nm (Chen and Massie, 1993). A scatterplot was made to show if there was any misclassification using reflectance, only four normal birds were classified as septicemic, one normal bird was classified as both septicemic and a cadaver, and six septicemic and five cadavers were classified as normal. This resulted in a 33% misclassification rate when the training set was observed, and the testing set

had a 5.6% in misclassification when using the reflectance model. Another scatterplot was made to show the interactance linear functions, this resulted in the rate of misclassification for wholesome carcasses to be 16.7% and for unwholesome carcasses to be 12.5% found in the testing set. Secondary difference scatterplots were made for each reflectance and interactance spectra, each showing less misclassification when observed. Overall, when reflectance spectra were used, a 94.4% accuracy for normal carcass classification was projected while a 93.1% accuracy classification was demonstrated for abnormal carcasses (Chen and Massie, 1993). When interactance spectra were used, 93.3% classification accuracy for normal carcasses and 96.2% accuracy for abnormal carcasses were displayed. Chen and Massie (1993) were able to successfully classify septicemic, cadavers, and normal carcasses with a diode-array spectrophotometer used at high-speed. This experiment using interactance used twenty-four wavelengths and had a probe that required to touch the carcass in order to gain a proper measurement. Although, results were ideal for an automated system, the procedure is limited on the execution of running at processing line speeds. The reflectance spectra did not require a probe for a point of contact with the carcasses and were able to narrow the use of four wavelength readings ranging from 500-850 nm (Chen and Massie, 1993).

Chao et al. (1999) examined chicken livers and hearts using a visible light/near-infrared (VIS/NIR) spectral camera. They worked with chicken livers and hearts that were separated into four classes, based on postmortem pathology, which were the following: normal, air sacculitis, cadaver, and septicemia. The images were taken with a white background and processed for morphological features and measurements of grey intensity (Chao et al., 1999). This experiment used feature extraction to help classify these organs. These images were processed using neuro-fuzzy based image classification algorithms where threshold values were depicted from

histogram intensities based on the images in each color space of red, green, and blue (RGB) (Chao et al., 1999). The fat band to total width band area ratio was used for the heart's classification while the gray-level intensities were averaged in RGB color space for the chicken liver classification (Chao et al., 1999). For statistical analysis, two models of neuro-fuzzy were used and 50% of the images were used for the training while the remaining 50% was used for the validation set. There were significant differences between the normal livers and the condemned carcasses when the RGB brightness values were compared. A significant difference was found between the cadaver and normal livers when paired similarly to the normal and air sacculitis livers when a Dunnett t-test was performed. There was not any significant difference found between the normal livers and the septicemic livers. When comparing the chicken hearts, there was significant differences between all four types. A Dunnett t-test was performed, showing significant differences between the normal and air sacculitis hearts as a pair and the normal and septicemic hearts. There was no significant difference found between the normal and cadaver hearts when compared. Results from the neuro-fuzzy model concluded with an 87.5% accuracy when using 50% of the data when comparing cadaver livers against normal livers (Chao et al., 1999). When RGB color was used for classification purposes for air sacculitis livers and normal livers, the results concluded a 92.5% accuracy for the validation set and 95% accuracy for the training set. For heart classification, the normal and air sacculitis samples resulted in % accuracy for the training set and 97.5 % accuracy for the validation set. The results for normal hearts and septicemic hearts were 95% accuracy for the training set and 92.5% accuracy for validation set. A four-class classifier was made to classify all four classes amongst another where spectral and spatial data was used, where the training set resulted in an 86.2 +/- 1% and the validation set had 82.5% accuracy (Chao et al., 1999).

Spectral imaging has been used to help identify carcass condemnations with the inspection of broiler chicken visceral organs but also with whole carcasses. Carcasses that were deemed to be cadavers, septicemia-toxemia, and air sacculitis were examined through spectral imaging for classification to begin the discussion of implementation of automated systems in poultry processing plants (Chen and Massie, 1993; Kim et al., 2006; Chao et al, 2007). The detection of fecal contamination on processing equipment has utilized spectral imaging given FSIS has a zero tolerance in processing plants before operation starts. Chao et al. (2007) used a hyperspectral-multispectral imaging system to locate the region of interest (ROI) on the breast of each carcass for determination of wholesome of unwholesome birds using line scan imaging. The ROI was the breast of the bird where line-scan images were taken at 400 images per second detecting the entry and exit of each carcass in the view of the camera that passed (Chao et al, 2007). Wavelength, 629 nm, was used for reflectance to detect the chicken carcass with a black background and using the hyperspectral camera using a total of fifty-five wavelengths for analysis. With a ROI boundary made, the pixels located in each image were used to form calibration sets taking the average highest and lowest values for each wholesome chicken for one set and systemically diseased for another (Chao et al., 2007). An image classification algorithm was developed on MATLAB using a fuzzy function using the ROI and significant wavelengths. As a result, they discovered using key wavelengths of 4 had the ability to perform quicker with data processing than using a higher number of wavelengths which were used for analysis (Chao et al, 2007). As a result of using the key wavelengths for the average fuzzy output calibration data set, when threshold was 40%, a 93.8% accuracy of unwholesome birds, where only four birds that were deemed unwholesome being misclassified, when plotted against the total number of ROI pixel values (Chao et al., 2007). When the systemically diseased birds were measured,

there was a 100% accuracy for correct classification and had 91.4% accuracy when off-shift imaged birds were removed. This resulted in an average of 96% accuracy for systemically diseased birds were classified correctly at 40% threshold. When threshold was increased, however, the differentiation accuracy for unwholesome and wholesome birds began to decrease. With systemically diseased birds being classified correctly, other condemnations were considered to be an issue in the industry. Fecal contamination has close association with foodborne pathogens which can be found on processing equipment surfaces, fruits, and meat carcasses (Park et al., 2005; Yang et al., 2010; Gorji et al., 2022). A spectral imaging system was used on post-harvest apples that were artificially inoculated with four different concentration levels of fecal matter from Holstein cows (Yang et al., 2010). A hyperspectral line-scan system utilizing violet LED excitation light was used for imaging once the apples were placed on a tray with a black background (Yang et al., 2010). Yang et al. (2010) developed an algorithm to detect the contaminated spots of the apple surfaces and not be recognized as a bruised spot for contamination. The fecal contamination spectra peaked at 680 nm in this observation (Yang et al., 2010). All fecal spots on the apples were able to be successfully identified through a multispectral algorithm model where the threshold was held at 89% while the highest accuracy percentage for both normal apples and contaminated apples together was only 92% (Yang et al., 2010). A hyperspectral imaging system was used in another study to detect fecal matter on hand-eviscerated broiler chicken carcasses. Cecal contaminants were collected from the ceca part of the digestive tract due to the consistency and color when compared to other digesta/fecal materials found in the digestive tract of chicken. Carcasses were cut in half to expose the internal visceral for this research for easier imaging (Park et al., 2005). Carcasses were hung on standard processing shackles and the imaging system sat on a transportable cart for ease of camera and

light adjustments. Line-scan images were taken of the clean carcass before contamination was placed on four areas that included fat, meat, bone, and inside shade of the carcass (Park et al., 2005). Images were analyzed and processed further to obtain a threshold, masked ratio, mask, and other components for comparison of clean and contaminated carcass halves (Park et al., 2005). Seven ROIs were used for on each carcass to detect where spectra peaks decreased for each contaminant spot and to determine a threshold for classification of contaminants. The percent accuracy varied from 75.9% to 96.95% when threshold values were 1.00 and 1.05 (Park et al., 2005). They concluded that the higher the threshold, the more contaminated carcasses were misclassified, although the imaging system was able to identify 92.5% accuracy of contaminated carcasses (Park et al., 2005). Although the method for this research was unconventional for the industry, given carcasses are not cut in half for processing, Park et al. (2005) were able to identify that cecal contamination can be detected on the outside and inside of chicken carcasses. A fluorescence imaging system was used in another research study examining raw meat carcasses to identify fecal contamination with a handheld camera system. This system differs from the other imaging system discussed in previous studies due to the flexibility and transporting ease of this camera. This multispectral camera utilizes LED lights to assist with ambient light brightness issues that were discovered in past research (Gorji et al., 2022). Raw skinned beef and sheep carcasses were video recorded at processing plants before chilling with this imaging system and removed from the processing line if deemed suspect for review of the inspectors on-hand. This research had two objectives: to identify fecal contamination on these carcasses and to differentiate contamination areas using a sematic segmentation algorithm on CNN models for further analysis. This research concluded that contaminated carcasses were detected when compared to clean carcasses at an accuracy rate of 97.32%, precision at 97.66%,

and recall at 97.06% (Gorji et al., 2022). When the sematic segmentation model was run to determine whether the segmented areas of fecal matter showed presence or absence, a different metric was used called intersection over union (IoU) to help with performance levels (Gorji et al., 2022). This produced these segmented fecal matter surfaces with an IoU of 89.34%, precision of 92.25%, and recall of 95.84% (Gorji et al., 2022). Gorji and team provided key research that fecal contamination can be detected with this handheld spectral imaging system. The conventional way of inspection can cause false negatives and even if contamination is caught, testing results in days of lab work. With implementing an automated system in processing plants, this reduces technical errors performed by plant workers and can provide beneficial inspection system for the industry.

DATA ANALYITICS

Multispectral imaging system. The optical imaging system called Contamination, Sanitation, Inspection, and Disinfection (CSI-D+) system (SafetySpect, Grand Forks, ND) was used for this study. Spectral imaging was captured through the settings that include multiple wavelength bands, a red, green, and blue (RGB) camera, an ultraviolet (UV) camera with an option of disinfection, and a LED setting for fluorescence. The disinfection setting was not utilized in this study. This system can be controlled by the screen on the camera or through a wireless connection to a computer or tablet placed within 20-30 ft of the camera. The displayed screen gives three modes to work the system where either a still image, video, or view finder modes can be exhibited and recorded on the desired connected device. Light Detection and Ranging (LIDAR) is used for measuring the distance between the CSI-D+ device and the surface that is being examined. Two of the RGB channels can be adjusted while fluorescence is in use. The green channel is a constant

while the red and blue channels can be adjusted. When the red channel is used, green color can be seen because the two wavelengths overlap. UV settings intentionally activated using special buttons on the camera can be used for disinfection. The LED light on the camera is used to induce fluorescence and can be intentionally activated. The LED light is combination of UV-A and UV-B light is used. The LED light cannot be altered and is set at 405nm when the RGB settings are used, and the LED light emits at 275nm when the UV-C LEDs are used. These lights are activated through electronic signals, being turned on and off by buttons. Materials can be detected using UV that are as low as 325-375 nm showing excitation of molecules. Certain parameters are used for the operation of the camera. (1) Exposure is how long the photo-sensitive cells are exposed to light that range from 0 to 350 milliseconds (ms). (2) Gain, measured in $1/100^{th}$ decibels or Millibels (mB), controls the sound or noise levels in background of images by adjusting the pixel activity. Gain changes the brightness of the background using an analog to digital converter. This allows the image to appear either more realistic or abstract. With more gain parameters set, however, more noise in the background will be present. (3) Brightness adds whiteness to the image. (4) Saturation changes the color intensity for display of the image. By reducing saturation, this helped the red, green, and blue channels to be more equivalent creating a more monochrome image. The blue channel can respond to 850 nm with red, which also overlaps into green. However, the red can see the green spectrum without any overlap of the two. The wavelength range for red is 500-565 nm and 660-735 nm for blue. (5) Hue adjusts the color tone intensity by rotating the chrominance field clockwise around its axis. (6) Gamma bends light to have darker or lighter values in image appear by controlling the linearity of the intensity response of the imaging system. (7) The red and blue balance (RB balance) is the last setting used. (8) The RB balance controls the red channel and blue

channel in the camera to give different illumination scenarios for best imaging results. Images produced are 1024 x 768 pixels in size which can be saved as either .jpg, .tiff, or .raw on the tablet.

Image Classification.

Convolution Neural Network. One of the models used in this experiment is called Convolution Neural Network, often called the CNN deep-learning model. The CNN model is derived from another system known as Artificial Neural Network (ANN) to develop the classification of images, segmentation of images, and for high performance and accuracy with object recognition (Ramdani et al., 2020; Ristiawanto et al., 2019). This is a supervised learning network that uses a deep learning algorithm that handles two-dimensional input data (Al-Saffar et al., 2017). This deep learning model can be used for image classification to provide knowledge elaborating on what one frame of food is portrayed as when using a food detection system (Ramdani et al., 2020).

The images were applied to the CNN model using Google Collaboration. Images were downloaded into Google Drive and separated by sessions of images were taken and into another folder by sep-tox and normal carcasses. An image analysis model was created for further image analysis using platform CUDA 11.2 and Pytorch machine learning framework with three ConvNet layers. Adam Optimizer (learning rate= 0.001, weight decay= 0.0001) with cross entropy loss function for training of model with fifty epoch which can be changed as required. There are three major steps that partake while working the CNN model. In the first step, the images were uploaded and placed into separate folders for normal and sep-tox carcasses. Images analyzed with this program underwent three major steps: picture collection, model configuration, and validation. In the first step, images were gathered for the base data where they are placed into appropriate folders

for identification. The next step was model configuration where CNN model uses iterative training to improve its identification accuracy (Wang et al., 2020). The pictures were augmented by resizing, rotations, and flipping. Seventy percent of the pictures that were uploaded were used for the training model, these images are classified as either normal or sep-tox. After classification, each image was augmented to reduce each picture to 150 x150, be vertically and horizontally flipped, and have a random rotation added to it. After being augmented, a test model was run using 20% of the remaining images to produce the best model or epoch for a validation test to ensure the model was accurate. The model was trained by the number of epochs, or iterations, that were selected by the user. The best model was selected through percent accuracy and tensor, which is used in the last decisive step and named the best test model. Tensor is a means of loss, the smaller the tensor produced, the higher the accuracy of classification will be when creating the best model for the validation step. The last step was the validation step where the best test model was run against an unidentified folder of the remaining images that were not used in the training set. This is where the CNN model uses the final 10% of images from a folder that has no identity specification of normal birds or sep-tox birds described and use the best selected test model created from the testing model. This validation model sorts those remaining images at random into their correct classification as best as possible. When the validation model is run, the convolution neural network model displays the categories in which they are classified. After prediction is performed, a data frame is created to calculate the class probabilities and percentages each image falls into place. The results are shown in a table format and a heat map is created for each individual image to show what percentage each image fell into the two classes represented in this research. Additionally, a heat map is created to display the overall classification map for each folder displaying which images are predicted into each class by percentage.

The images were classified using a second method, Custom Vision AI which is a supervised image classification system. This system uses the Microsoft Azure platform to help train a custom multi-class image classification using machine learning techniques in real time through a CNN algorithm. Microsoft Custom Vision provides models that cultivates detection, segmentation, and classification (Andriyanov et al., 2023). Images were uploaded in appropriate folders and trained. After training, a performance was run on the images for accuracy of classification. This system scales probability threshold and depicts the precision, recall, and accuracy percentage (AP). The precision measures the percentage of the model selected on how accurate it will predict images to their respective tags. The recall shows all tag outcomes and the correct predictability percentage the model correctly places each image within these tags. The AP is the measure of the model performance which outlines the precision and recall at different thresholds and shown through percentage accuracy. The threshold can change the predictable probability of images into the correct tag. The threshold ranges from 0 to 100%, where the default threshold is 50%. After training has occurred, there is a probability threshold that administers the minimum probability score for a prediction validity during classification of the images when calculating precision and recall. After the model has been trained, images that are to be tested can be run with the trained model and computes the percentage probability for the image to be classified under each tag. There is an additional test that can be run for individual pictures to determine the percent the image categorized under each tag.

The results were shown in a table format and a heat map is created for each individual image to show what percentage each image fell into the two classes represented in this research. Additionally, a heat map is created to display the overall classification map for each folder displaying which images are predicted into each class by percentage.

CONCLUSION

Rapid detection is able to help identify these foodborne pathogens in a quicker and more illustrated manner like the spectral technique that was able to produce results in five to fifteen minutes (Michael et al., 2019). With spectral technologies like this, it will help the improvement of the detection of bacterial contamination in poultry processing plants. For future studies in identifying bacteria, spectral detection is a positive and upcoming method used through multi-scaled industries. With processing lines ran at high speeds, spectral imaging must be suitable to the fast pace of the line and can execute tactful low-light imaging successfully for online use in processing plants. One of the benefits of multispectral imaging to the industry is providing an easier process to detect bacteria on food and equipment surfaces, fecal contamination of meat products and produces, or organic residues found on processing equipment compared to cultural methods that are currently set in place if PCR is not currently in use at facilities. The evisceration line would be fed only wholesome birds, allowing for higher speed processing lines while minimizing food safety risks and cross-contamination of equipment (Park et al., 2005; Chao et al., 2007). Implementing spectral imaging into poultry processing plants to adhere with the unwavering speed of production lines can alleviate some missed contaminated carcasses that spread foodborne pathogens to consumers.

REFERENCES

Alamer, S., S. Eissa, R. Chinnappan, and M. Zourob. 2018. A Rapid Colorimetric Immunoassay for the Detection of Pathogenic Bacteria on Poultry Processing Plants using Cotton Swabs and Nanobeads. Microchimica Acta 185.

Anderson, J., C. Reynolds, D. Ringelberg, J. Edwards, and K. Foley. 2008. Differentiation of Live-Viable Versus Dead Bacterial Endospores by Calibrated Hyperspectral Reflectance Microscopy. Journal of Microscopy 232:130–136.

Andriyanov, N., Y. Kamalova, and V. Dementiev. 2023. Comparison of MS Custom Vision Auto Machine Learning with Algorithms Implementation Methods. 2023 Wave Electronics and its Application in Information and Telecommunication Systems (WECONF).

Bharmoria, A., A. Shukla, and K. Sharma. 2017. Typhoid fever as A Challenge for Developing Countries and Elusive Diagnostic Approaches Available for the Enteric Fever. International Journal of Vaccine Research 2:1–16.

Centers for Disease Control and Prevention (CDC). 2021a. *Salmonella* homepage. Centers for Disease Control and Prevention Available at https://www.cdc.gov/salmonella/index.html (verified 10 November 2021).

Centers for Disease Control and Prevention (CDC). 2021b. *Listeria* (listeriosis). Centers for Disease Control and Prevention Available at https://www.cdc.gov/listeria/index.html (verified 24 October 2021).

Chao, K. 2010. Online inspection. Handbook of Poultry Science and Technology:683–701. ((Chao, K. 2010. "Online Inspection." In I. G. Legarreta and Y. H. Hui, edited by. Handbook of Poultry Science and Technology (Vol. 1). NJ, USA: Primary Processing. John Wiley & Sons; 683–701.))

Chao, K., Y.R. Chen, H. Early, and B. Park. 1999. Color Image Classification Systems for Poultry Viscera Inspection. Applied Engineering in Agriculture, 15:363–369.

Chao, K., S. Dhakal, W. F. Schmidt, J. Qin, M. Kim, Y. Peng, and Q. Huang. 2020. Raman and IR Spectroscopic Modality for Authentication of Turmeric Powder. Food Chemistry 320:126567.

Chen, Y. R., and D. R. Massie. 1993. Visible/Near-Infrared Reflectance and Interactance Spectroscopy for Detection of Abnormal Poultry Carcasses. Transactions of the ASAE 36:863–869.

Eady, M., and B. Park. 2021. An Unsupervised Prediction Model for Salmonella Detection with Hyperspectral Microscopy: A Multi-Year Validation. Applied Sciences 11:895.

Eady, M., B. Park, and S. Choi. 2015. Rapid and Early Detection of Salmonella Serotypes with Hyperspectral Microscopy and Multivariate Data Analysis. Journal of Food Protection 78:668–674.

Eady, M., G. Setia, and B. Park. 2019. Detection of Salmonella from Chicken Rinsate with Visible/Near-Infrared Hyperspectral Microscope Imaging Compared against RT-PCR. Talanta 195:313–319.

Fontanot, M., L. Iacumin, F. Cecchini, G. Comi, and M. Manzano. 2014. Rapid Detection and Differentiation of Important *Campylobacter* Spp. in Poultry Samples by Dot Blot and PCR. Food Microbiology 43:28–34.

Fronczek, C. F., D. J. You, and J.-Y. Yoon. 2013. Single-Pipetting Microfluidic Assay Device for Rapid Detection of Salmonella from Poultry Package. Biosensors and Bioelectronics 40:342–349.

Gallagher, D. L., E. D. Ebel, and J. R. Kause. 2003. Draft FSIS Risk Assessment for *Listeria* in Ready-to-Eat Meat and Poultry Products. Federal Register :Request Access Available at https://www.federalregister.gov/documents/2015/06/19/2015-13507/control-of-listeria-monocytogenes-in-ready-to-eat-meat-and-poultry-products (verified 2 December 2021).

Gorji, H. T., S. M. Shahabi, A. Sharma, L. Q. Tande, K. Husarik, J. Qin, D. E. Chan, I. Baek, M. S. Kim, N. MacKinnon, J. Morrow, S. Sokolov, A. Akhbardeh, F. Vasefi, and K. Tavakolian. 2022. Combining Deep Learning and Fluorescence Imaging to Automatically Identify Fecal Contamination on Meat Carcasses. Scientific Reports 12.

NCI of Health (Health). 2021. NCI Dictionary of Cancer terms. Comprehensive Cancer Information - NCI Available at https://www.cancer.gov/publications/dictionaries/cancer-terms/def/immunoassay (verified 2 December 2021).

Joo, J., C. Yim, D. Kwon, J. Lee, H. H. Shin, H. J. Cha, and S. Jeon. 2012. A Facile and Sensitive Detection of Pathogenic Bacteria using Magnetic Nanoparticles and Optical Nanocrystal Probes. The Analyst 137:3609.

Kim, M. S., A. M. Lefcourt, and Y.-R. Chen. 2003. Optimal Fluorescence Excitation and Emission Bands for Detection of Fecal Contamination. Journal of Food Protection 66:1198–1207.

Kim, M. S., Y.-R. Chen, S. Kang, I. Kim, A. M. Lefcourt, and M. Kim. 2006. Fluorescence Characteristics of Wholesome and Unwholesome Chicken Carcasses. Applied Spectroscopy 60:1210–1216.

Lawrence, L. M., and A. Gilmour. 1994. Incidence of *Listeria* Spp. and *Listeria monocytogenes* in a Poultry Processing Environment and in Poultry Products and their Rapid Confirmation by Multiplex PCR. Applied and Environmental Microbiology 60:4600–4604.

Michael, M., R. K. Phebus, and J. Amamcharla. 2019. Hyperspectral Imaging of Common Foodborne Pathogens for Rapid Identification and Differentiation. Food Science & Nutrition 7:2716–2725.

National Chicken Council (NCC). 2022. Broiler Chicken Industry Key Facts 2021. National Chicken Council Available at https://www.nationalchickencouncil.org/about-the-industry/statistics/broiler-chicken-industry-key-facts/ (verified 2 December 2021).

Park, B., K. C. Lawrence, W. R. Windham, and D. P. Smith. 2005. Detection of Cecal Contaminants in Visceral Cavity of Broiler Carcasses using Hyperspectral Imaging. Applied Engineering in Agriculture 21:627–635.

Peng, Y. T., and S. Dhakal. 2015. Optical Methods and Techniques for Meat Quality Inspection. Transactions of the ASABE:1371–1386.

Qin, J., Chao, K., Kim, M. S., Kang, S., Cho, B.-K., and Jun, W. 2011. Detection of Organic Residues on Poultry Processing Equipment Surfaces by LED-Induced Fluorescence Imaging. Applied Engineering in Agriculture, 27:153–161.

Ramdani, A., A. Virgono, and C. Setianingsih. 2020. Food Detection with Image Processing using Convolutional Neural Network (CNN) Method. 2020 IEEE International Conference on Industry 4.0, Artificial Intelligence, and Communications Technology (IAICT).

Ristiawanto, V., B. Irawan, and C. Setianingsih. 2019. Wood Classification with Transfer Learning Method and Bottleneck Features. 2019 International Conference on Information and Communications Technology (ICOIACT).

Robert-Rössle-Strasse. 2021. Home. CONGEN Available at https://www.congen.de/en/ (verified 1 December 2021).

Robinson, S. 2018. The Big Five: Most Common *Salmonella* Strains in Foodborne Illness Outbreaks. Food Safety News. Available at https://www.foodsafetynews.com/2013/08/the-five-most-common-salmonella-strains/ (verified 6 September 2022).

Romero, M. R., and N. Cook. 2018. A Rapid Lamp-Based Method for Screening Poultry Samples for *Campylobacter* without Enrichment. Frontiers in Microbiology 9.

Scallan, E., R. M. Hoekstra, F. J. Angulo, R. V. Tauxe, M.-A. Widdowson, S. L. Roy, J. L. Jones, and P. M. Griffin. 2011. Foodborne Illness Acquired in the United States—Major Pathogens. Emerging Infectious Diseases 17:7–15.

Sueker, M., K. Stromsodt, H. T. Gorji, F. Vasefi, N. Khan, T. Schmit, R. Varma, N. Mackinnon, S. Sokolov, A. Akhbardeh, B. Liang, J. Qin, D. E. Chan, I. Baek, M. S. Kim, and K. Tavakolian. 2021. Handheld Multispectral Fluorescence Imaging System to Detect and Disinfect Surface Contamination. Sensors 21:7222.

Sun, Q., G. Zhao, and W. Dou. 2015. Blue Silica Nanoparticle-Based Colorimetric Immunoassay for Detection of Salmonella pullorum. Anal. Methods 7:8647–8654.

Super, T. 2018, July 24. Survey Shows Us Chicken Consumption Remains Strong. National Chicken Council. Retrieved November 24, 2021, from https://www.nationalchickencouncil.org/survey-shows-us-chicken-consumption-remains-strong/.

United States Department of Agriculture Food Safety and Inspection Service (USDA-FSIS). 2014a. Food Safety and Inspection Service. Modernization of Poultry Slaughter Inspection | Food Safety and Inspection Service Available at https://www.fsis.usda.gov/policy/federal-register-rulemaking/federal-register-rules/modernization-poultry-slaughter (verified 4 February 2024).

United States Department of Agriculture Food Safety and Inspection Service (USDA-FSIS). 2014b. "Compliance Guideline for Training Establishment Carcass Sorters in the New Poultry Inspection System (NPIS)." FSIS-GD-2014-0013. https://www.fsis.usda.gov/guidelines/2014-0013.

United States Department of Agriculture Food Safety and Inspection Service (USDA-FSIS). 2019. Verification of Procedures for Controlling Fecal Material, Ingesta, and Milk in Livestock Slaughter Operations. FSIS Directve 6420.2 revision 2 Available at https://www.fsis.usda.gov/sites/default/files/media_file/2020-07/6420.2.pdf (verified 21 November 2021).

United States Department of Agriculture Food Safety and Inspection Service (USDA-FSIS). 2023. Microbiology Laboratory Guidebook. Microbiology Laboratory Guidebook | Food Safety and Inspection Service Available at https://www.fsis.usda.gov/news-events/publications/microbiology-laboratory-guidebook (verified 22 November 2021).

United States Department of Agriculture National Agricultural Statistics Service (USDA-NASS). 2024. USDA Economics, Statistics and Market Information System. Available at https://usda.library.cornell.edu/.

Wachiralurpan, S., T. Sriyapai, S. Areekit, T. Kaewphinit, P. Sriyapai, S. Santiwatanakul, and K. Chansiri. 2017. Development of a Rapid Screening Test for Listeria monocytogenes in Raw Chicken Meat using Loop-Mediated Isothermal Amplification (LAMP) and Lateral Flow Dipstick (LFD). Food Analytical Methods 10:3763–3772.

Wang, D., F. Tian, S.X.Yang, Z. Zhu, D. Jiang, and B. Cai. 2020. Improved Deep CNN with Parameter Initialization for Data Analysis of Near-Infrared Spectroscopy Sensors. Sensors, 20:874.

Wold, J. P., F. Lundby, and B. Egelandsdal. 1999. Quantification of Connective Tissue (Hydroxyproline) in Ground Beef by Autofluorescence Spectroscopy. Journal of Food Science 64:377–383.

Yang, C.-C., M. S. Kim, S. Kang, T. Tao, K. Chao, A. M. Lefcourt, and D. E. Chan. 2010. The Development of a Simple Multispectral Algorithm for Detection of Fecal Contamination on Apples using a Hyperspectral Line-Scan Imaging System. Sensing and Instrumentation for Food Quality and Safety 5:10–18.

Yang, Q., H. Xu, Y. Zhang, Y. Liu, X. Lu, X. Feng, J. Tan, S. Zhang, and W. Zhang. 2020. Single Primer Isothermal Amplification Coupled with SYBR GREEN II: Real-Time and Rapid Visual Method for Detection of *Listeria monocytogenes* in Raw Chicken. LWT 128:109453.

CHAPTER II.

Identification and Classification of Broiler Carcasses Exhibiting Septicemia-Toxemia using Spectral Imaging Systems

Abstract

Septicemia-toxemia (sep-tox) is a bacterial infection in the bloodstream of live broilers which can result in red carcasses, dehydrated skin, or organ hemorrhaging. During processing, USDA inspectors or trained plant personnel visually inspect broiler carcasses and separate those exhibiting sep-tox characteristics, which can be a fatiguing process. With the potential of increasing processing line speeds, it is appropriate to develop innovative real-time technologies to detect sep-tox. We investigated an RGB color imaging spectral camera system combined with machine learning for the detection of sep-tox carcasses. A total of 380 carcasses, identified as sep-tox by trained plant personnel or USDA inspectors, and 286 non-sep-tox (market ready) carcasses were procured from a commercial poultry processor in twelve separate trials. Each carcass was placed in a cabinet to prevent ambient light from interfering with imaging. The CSID+ imaging system (SafetySpect) was used for collecting two images per carcass at different exposure times to obtain a total of 1,332 images. Image analysis using data analytics was conducted with a supervised learning network, convolution neural network, to categorize images into normal and sep-tox. The convolution neural network was able to validate the picture with a ninety-eight percent training accuracy and a one-hundred percent testing accuracy average using the best model this network produced. Custom Vision was used for classification at two thresholds, fifty and eighty-five percent, resulting in 100 percent accuracy for all images in their respective class. RStudio was run on only sep-tox images to receive a scatterplot showing diversity between septox images. The scatterplot resulted in close knit clusters, but clusters were distinguishable resulting in 252 images in cluster one, 146 images in cluster two, and 214 images in cluster three. The spectral camera was effective in detecting septicemia-toxemia in broiler

carcasses in a laboratory setting and can be further investigated for its application in the processing environment.

Introduction

Poultry is the most popular meat consumed across the world with the consumption rates almost doubling over the past two decades (OECD, 2017). In the US alone, there has been a 20% increase in chicken consumption over the last twenty years which has reached 98.0 lbs. per capita in 2021 (USDA-FSIS, 2022). Although popular, consumers are concerned about the safety of poultry and the foodborne diseases associated with it (Super, 2018). Hence, there are significant efforts taken by the poultry industry and government regulators to ensure safety and wholesomeness of poultry meat.

Broiler carcasses are inspected individually in processing plants for several defects or condemnations that may render the meat unsafe and unwholesome which will lead to degradation of meat quality or discarding of the carcass. At a commercial poultry processing plant, the inspection is overseen by USDA-Food Safety and Inspection Service (FSIS) inspectors, along with trained plant workers, who are placed along the processing line near the evisceration station inspecting each chicken carcass that is processed. The inspectors conduct visual and physical inspection of both the carcass and the viscera that have been extracted from that particular carcass (Chao, 2010). Inspection includes examining the external surface of the carcass, the internal cavity surfaces, and all organs of the carcass to identify any of the prescribed reasons for carcass condemnations such as fecal contamination, air sacculitis, septicemia-toxemia among others. Carcasses affected by certain contaminations such as fecal contamination

are reprocessed as per the prescribed method and rehung for next steps in processing. However, certain other defects render the carcass unfit for human consumption and must be condemned.

One such carcass defect that results in condemnation that is prominent in the poultry processing industry is called septicemia-toxemia. Septicemia-toxemia is the number one named cause of carcass condemnations observed in the poultry industry (USDA-NASS, 2024). With more than nine billion chickens being produced a year on average, this is an issue as it results in an overall yield loss (USDA-FSIS, 2021). Septicemia-toxemia, commonly referred to as sep-tox, encompasses septicemia, a bacterial infection that enters the bloodstream due to pathogenic microorganisms or their toxins, and toxemia, a localized infection resulting from toxins produced by cells or the proliferation of microorganisms (Chao et al., 2008). Signs of sep-tox on carcasses are a range of red, dark red to bluish color to the appearance of the carcass and can have excessive fluid in the chest cavity (Dey et al., 2003). The red appearance is produced from petechial hemorrhages to the liver, heart, kidney, muscle, and membranes. Another common sign in chicken is inflammation of organs such as the liver, spleen, and kidneys (Chao et al., 1999). Sep-tox birds are smaller in size and have a dehydrated look with potentially stunted growth (USDA-FSIS, 2014). Although septicemia-toxemia is an infection in the bloodstream, in some cases it cannot be seen before processing the broiler chicken. This illness can have a full recovery from the bacterial infection but over time, if not treated, can be fatal to the infected bird. The infected chickens are deemed unsafe for human consumption and discarded (USDA-FSIS, 2014). Birds that develop septicemia-toxemia are prohibited by federal regulation and occur in less than 0.2% of the chickens that are processed (Chao et al., 2007) which extrapolates to 18 million broilers of the 9 billion produced every year in the US.

In a processing plant, the USDA inspector or a trained plant personnel visually identify a sep-tox affected carcass and remove it from the processing line legally allowed to be run at 140-175 birds per minute (bpm) (Chao et al., 2004). The processing line speed, combined with personnel bias and fatigue could result in the detection of false negative or false positive sep-tox carcass identification leading to either unwholesome carcasses entering the food chain or economic losses, respectively. However, HACCP-based inspection models project (HIMP) of the USDA-FSIS requirements includes a zero tolerance for unwholesome chickens demonstrating symptoms of sep-tox (Chao, 2010; Dey et al., 2003). Hence rapid sep-tox carcass detection technologies which can allow for an accurate and repeatable detection of affected carcasses while aiding trained workers doing their laborious job would be beneficial to the poultry industry and regulators.

A spectral camera can use wavelength bands of red, green, and blue (RGB), ultraviolet light (UV), and LED settings for fluorescence on the chicken carcasses on processing lines to identify the carcass defects. Multiple spectral imaging systems have been researched for automation inspection with the goal of implementation into poultry systems. Research using spectral imaging was conducted by Dey et al. (2003) on chicken livers from birds diseased with septicemia. These organs were examined with visible light/near-infrared (vis/NIR) spectroscopy to record any physical or chemical changes that have occurred for rejection under the HIMP criteria using pattern recognition from both healthy and infected livers. They observed a significant spectral difference between the normal and sep-tox livers at 750 nm for visible light and 2,300 nm for infrared light. Chao et al. (2004) successfully demonstrated the effectiveness of a transportable vis/NIR spectroscopy data acquisition and processing capability at a high

throughput processing facility at 70-90 birds per minute to classify birds at wholesome and unwholesome.

Over the years, steps into using spectral imaging have progressed from line scan imaging systems to a more readily accessible system. Sueker et al. (2021) performed a study with a handheld spectral camera, CSI-D, for the rapid detection of saliva and respiratory droplets, along with other organic residues, on stainless steel and plastic surfaces that are present daily in food processing facilities and kitchens. The CSI-D system captures the presence and absence of contamination using different variations of UV light. This type of CSI-D camera system may also have useful applications within the poultry processing industry.

The objective of the study performed was to use a fluorescent multi-spectral imaging system to facilitate the identification of processed chicken carcasses that exhibit septicemia-toxemia using an image classification method system based on supervised and unsupervised deep learning algorithms for further image analysis.

Materials and Methods

Experimental Design.

To help reduce errors in identifying sep-tox chicken, twelve sessions were performed using the CSI-D+ system in a laboratory setting to capture images. A box was configured with two black forty-five-gallon polypropylene tote containers (20.8 in. L x 45.2 in. W x 18.9 in. H) (Rubbermaid, Atlanta, GA) a plain steel cold rolled round rod (1/8 in. x 36 in.), and a poultry shackle to hang the chicken carcasses for imaging shown in Figure 2.1. The box was essential to limit any ambient light interference and for a more controlled background in the images. A camera stand (9.5 in. L x 7.2 in. W x 6.2 in. H) was built to keep the carcasses within the camera's view once placed on the shackle. CSI-D+ was set up and placed inside the box on the

stand, twelve inches (30.48 cm) away from the breast of the chicken carcass hung on the shackle. The carcasses were placed inside the box onto the poultry shackle and images were taken using the RGB setting. Broiler chicken carcasses were processed and received from a USDA-inspected commercial poultry processing plant and brought to the Department of Poultry Science, Auburn University in coolers on ice. Broiler carcasses identified as sep-tox by either the USDA-FSIS personnel or the trained plant personnel and those deemed wholesome (normal) were received from the processor. The first four imaging sessions involved a total of 160 chicken carcasses with an average of forty chicken carcasses per session (Table 2.1). The next six sessions (5-10) contained 395 chicken carcasses with approximately thirty carcasses per session, (Table 2.1). A total of 790 images were captured with a resolution of 1024 x 768 pixels. The last two sessions (11-12) were performed at the poultry processing plant where only carcasses deemed systemically diseased with sep-tox from processing plant workers were photographed. The ambient light free box was transported to the processing plant and used for imaging. In total, 111 birds that were deemed to have sep-tox were collected, resulting in 222 images captured with two exposure times, 230ms and 270ms, and a resolution of 1024 x 768 pixels. Images were uploaded onto a computer and used for further analysis on Google Collaboration, Azure Custom Vision, and R Studio for image classification.

Figure 2.1. Experimental design of camera set up to remove ambient light.

Table 2.1. Summary of sessions displaying the number of carcasses and carcass images taken with camera parameters listed in Table 2.2.

Carcass Sessions and Parameters				
Session No.	Septox no.	Normal no.	Images Taken	Camera Parameters used
1	24	24	96	A
2	10	23	66	A
3	20	20	80	A
4	20	19	78	A
5	21	16	74	B
6	20	16	72	B
7	20	18	76	B
8	68	50	236	B
9	33	50	166	B
10	33	50	166	B
11	64	0	128	B
12	47	0	94	B

Multispectral Imaging System.

The optical imaging system called Contamination, Sanitation, Inspection, and Disinfection (CSI-D+) system (SafetySpect, Grand Forks, ND) was used for the study. This

system was controlled by a wireless connection to a tablet placed within 20-30 ft of the camera. The displayed screen gives three modes to work the system where either a still image, video, or view finder mode can be exhibited and recorded on the desired connected device. For this experiment still images were selected. Light Detection and Ranging (LIDAR) was used for measuring the distance between the CSI-D+ device and the surface that was being examined to determine the proximity of the chicken carcass to the camera. Two of the RGB channels were adjusted while fluorescence was in use. The LED light on the camera induced fluorescence and was intentionally activated. The LED light was a combination of UV-A and UV-B light and was set at 405nm when the RGB settings were used in this experiment. Two different sets of camera parameters were used in this study in Table 2.2. The first four imaging sessions (sessions 1-4) utilized camera setting A (Table 2.2) Exposure times were set at 175 and 350 ms. Gain was set at 1296 mB and brightness was set at 11. Saturation was set to 166 and gamma settings were placed at 145. The red balance was set to 4741 while the blue balance was set to 0. Due to oversaturation of images taken with setting A, camera parameters were adjusted for the remaining sessions (5-12) and are labeled as setting B (Table 2.2). For setting B's parameters, the exposure times were at 230 and 270 ms. Gain was set to 1000 mB and the brightness was reduced to 3. The saturation decreased to 45 and hue was set to 0. The gamma was set to 80 while both red and blue balance were set to 4000. Images produced were 1024 x 768 pixels in size and were saved as either .jpg or .tiff on the tablet.

Image Classification.

Google Collaboration. All of the images were applied to a CNN model using Google Collaboration. An image analysis model was created using platform CUDA 11.2 and Pytorch

machine learning framework with three ConvNet layers. Adam Optimizer (learning rate= 0.001, weight decay= 0.0001) was used with cross entropy loss function for training of model with fifty epochs which was changed as needed. Three major steps occurred while working the CNN model: picture collection, model configuration, and validation. In the first step, the images were uploaded and placed into separate folders for normal and sep-tox carcasses. The next step was model configuration where the CNN model used iterative training to improve its identification accuracy (Wang et al., 2020). Seventy percent of the pictures that were uploaded were used for the training model and these images were classified as either normal or sep-tox. The pictures were augmented by resizing to 150 x 150 pixels, rotated randomly, and flipped vertically and horizontally after classification occurred. After being augmented, for the third step, a test model was run using 20% of the remaining images to produce the best model or epoch for a validation test to ensure the model was accurate. The model was trained by the number of epochs, or iterations, that were selected by the user. The best model was selected through highest percent accuracy and tensor, which was used in the last decisive step and named the best test model. The last step was the validation step where the best test model was run against an unidentified folder of the remaining images that were not used in the training set. The CNN model used the final 10% of images from a folder that had no identity specification of normal birds or sep-tox birds described and used the best selected test model created from the testing model. This validation model sorted the remaining images at random into their correct classification. When the validation model was run, the convolution neural network model displayed the categories in which they were classified. After prediction performance, a data frame was created to calculate the class probabilities and percentages to display where each image was classified.

Custom Vision AI. The images were classified using a second method, Custom Vision AI, which is a supervised image classification system. This system was used to help train a custom multi-class image classification using machine learning techniques in real-time through a CNN algorithm for the normal carcass and sep-tox images. Images from sessions 5-12 only were uploaded in appropriate folders and trained. After training, a performance was run on the images for accuracy of classification. This system scales the probability threshold and depicts the precision, recall, and accuracy percentage (AP). The precision measures the percentage of the model selected on how accurate it will predict images to their respective tags. The recall shows all tag outcomes and the correct predictability percentage the model correctly places each image within these tags and the AP is the measure of the model performance which outlines the precision and recall at different thresholds and is shown through percentage accuracy. After training has occurred, there is a probability threshold used at 50 and 85 percent. After the model was trained, images were tested with the trained model and the percentage probability for the images was classified under each tag.

RStudio. The third machine learning program used in this experiment was unsupervised learning using RStudio version 2.1.4. A code was generated using the Artificial Intelligence Machine-Learning (AI-ML) ChatGPT 3.5 (OpenAI, San Francisco, CA) to separate and evaluate the familiarity or differences between the carcasses deemed septicemia-toxemia by using k-means clustering and principal components. The images used for RStudio were the sep-tox images from sessions 5-12. Libraries, described below, were downloaded and used to help evaluate the images and separate them into clusters. To create the scatterplot, “ggplot2” was added to the system’s library. The library “jpeg” used either name of the file (jpg, jpeg) to read from a raw vector representing the JPEG file content that was used in the selected folder. All

images were converted to their respectable files so cluster formation could use all images. The library “cluster” was used to help sort each image uploaded into the database and placed into respective groups through similarities between the images. To help develop the clusters that were picked for the R code used, principal component analysis was performed for an unsupervised analysis of the linear components of each image to better visualize the small variables that were present within the dataset without any associated Y component (Boehmke, 2018). Before getting the principal components, the images were extracted, nulled, standardized, and an analysis was run to determine the principal component analysis. After all image features were selected, the type of image was described in the codes using “.jpg” and “.jpeg” that was recognized as a regular expression pattern for files that end in either “.jpg” and “.jpeg” and were matched together for selection of files. An image file was created on R to extract features or values from all images placed inside the image directory for image analysis. A matrix file was created for the features to help remove any duplicate features that were stored. The data collected in the matrix was standardized for clustering by organizing the image matrices in order. The scaled matrix consisted of 612 images with 50 vectors. With the surplus of vectors produced, the first two vectors were only used for clustering. A total of three clusters were chosen for differentiation of levels of sep-tox with k-means clustering. A file was made to help extract features from the images that included any null or undefined values. The null values were removed from the image features file and the image file. With the null values discarded, the data were standardized, and k-means clustering was performed again for a more accurate demonstration of variation between septicemia-toxemia in the images that were collected. The cluster assignments created were reintroduced to the original data where a bar plot was created to show variation in sep-tox carcasses where k-means clustering was implemented. Principal components analysis (PCA) was

performed on the scaled matrix data. The first two main components were used with the cluster assigned groups to create a scatterplot for the images. The standard deviation for the first principal component was 15.07 and the second principal component's standard deviation was 12.61. These two principal components and the clustered data collected earlier were collectively added to the original data to compute a desired scatterplot.

Table 2.2. CSI-D+ camera parameters utilized for all sessions, where the settings for sessions 1-4 are recognized as A, and the reframed parameters in sessions 5-12 are recognized as B.

Camera Parameters	Sessions 1-4 (A)	Sessions 5-12 (B)
LED	405nm	405nm
Exposure	175ms; 350ms	230ms; 270ms
Gain	1296mB	1000mB
Brightness	11	3
Saturation	166	45
Hue	-1165	0
Gamma	145	80
Red Balance	4741	4000
Blue Balance	0	4000

Results and Discussion

The first camera settings (A) resulted in a total of 160 carcasses, sep-tox (n=74) and normal (n=86), being used over four sessions of image capturing (Table 2.1). Images from sessions 5-12 (B) were run with the CNN supervised learning models with 306 sep-tox and 200 normal carcasses resulting in 506 total.

Sessions 1-4. The sep-tox carcasses appeared red in the images while the normal carcasses were yellow in appearance with the initial settings used and are shown in Figure 2.2. These images were cropped to remove the excess background. Carcass images were classified with the CNN Google Collaboration resulting in 98% accuracy for the training and testing models, while

resulting in 100% accuracy for the validation model. With the camera settings used (A), there was an excessive amount of saturation on the carcasses photographed. After reviewing the images, new camera setting parameters were set to create more efficient images for classification (Table 2.2, B). The images from sessions 1-4 were not used for further analysis and were removed from the data set.

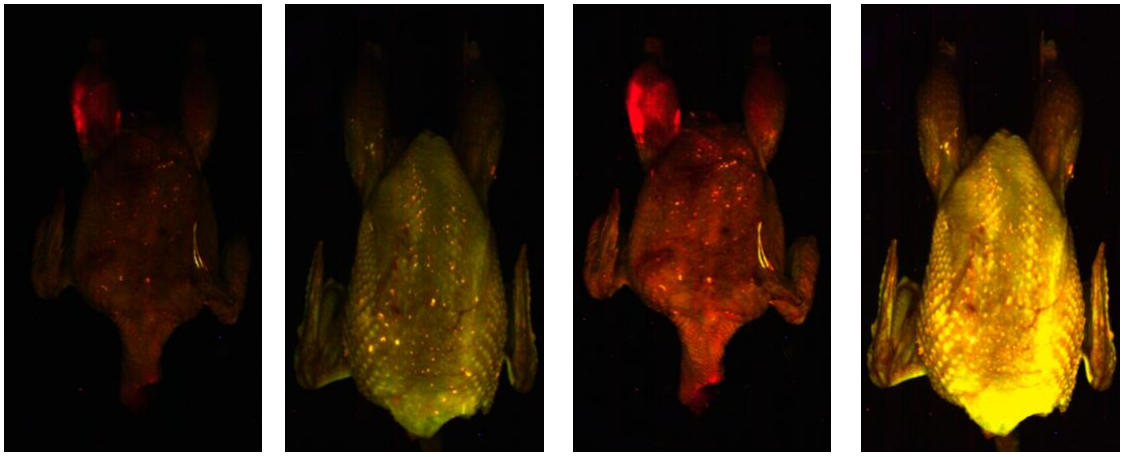

(a) (b) (c) (d)

Figure 2.2. Spectral images of sep-tox and normal carcasses taken at exposure times of 175 ms (a-b) and 350 ms (c-d) at initial setting A used for sessions 1-4, showing oversaturation.

Sessions 5-10. Subsequent sessions 5-10 were conducted with 506 chicken carcasses over six sessions, where 306 septox birds and 200 normal chicken carcasses were photographed resulting in 1,012 images taken. There was a visible difference between the sep-tox carcass and normal carcass in the images shown in Figure 2.3. The normal carcasses appeared pale with some white reflectance on the breast area. The sep-tox carcasses were red in appearance and only displayed reflectance from missed cuticle skin due to processing. The configured CNN model demonstrated 100% accuracy in training, testing, and validation results. A heat map was created upon classification showing that 52% of images were placed into the normal class and 48% of

images were placed into the sep-tox class (Figure 2.4). The individual classification heatmap shows that all images in the testing model were placed 100% into their correct classification.

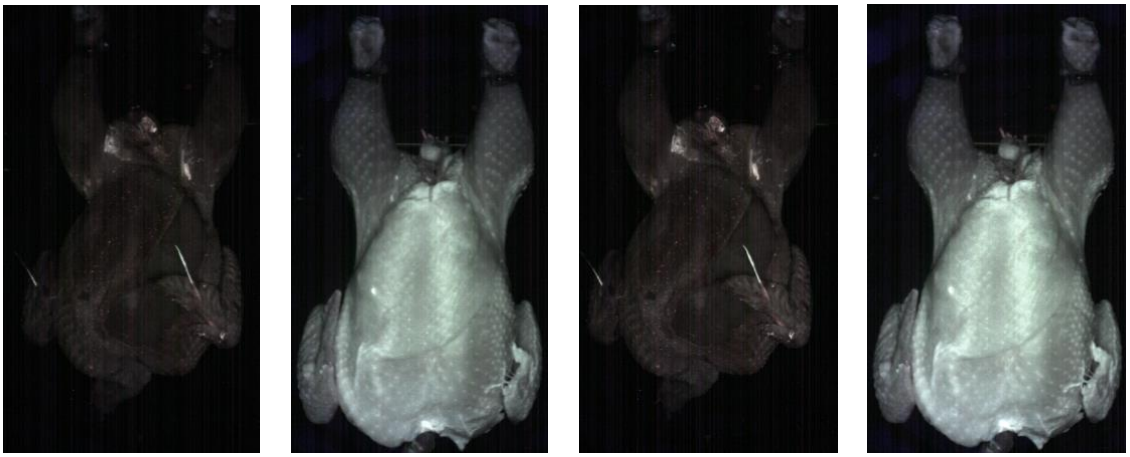

(a) (b) (c) (d)

Figure 2.3. Spectral images of sep-tox and normal carcasses taken at exposure times of 230 ms (a-b) and 270 ms (c-d) with updated camera parameters B, sessions 5-12, for grey-scale imaging.

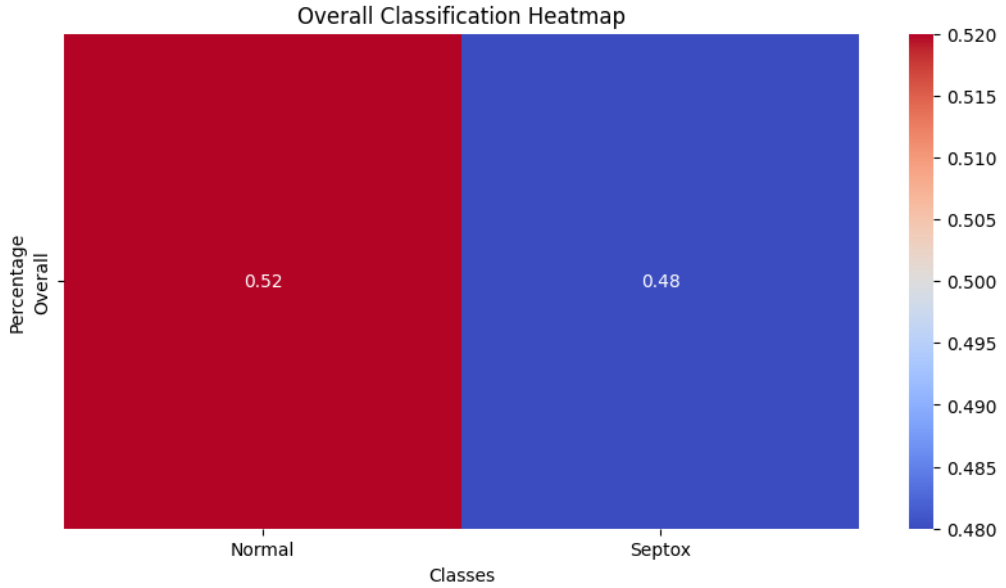

Figure 2.4. Heatmap for overall classification of sep-tox and normal carcass images from sessions 5-12.

Microsoft Custom Vision is a supervised learning machine that determined at a threshold of 50%, the precision, recall, and accuracy percentage and was able to classify all images at

100% accuracy. To get a better understanding in the accuracy of this system, the threshold was placed at 85%, where the precision was 100%, recall was 96.6%, and the AP was 100% for overall classification (Table 2.3). The recall had a 96.7% accuracy of proper classification for sep-tox and a 96.3% for normal carcasses in their respective classes. Four images from the sep-tox class and three images from normal class did not meet the 85% threshold probability prediction for recall. This image classification system was able to accurately identify all images in their respective tags, “Septox” and “Normal” though the probability scores in recall did not predict that in the 85% threshold. Providing aide for the processing plant workers and USDA inspectors with their task of identifying sep-tox birds can be beneficial with this camera used in the poultry processing plants for assisting with inspection of carcass condemnations such as septicemia-toxemia.

Table 2.3. Microsoft Custom Vision classification accuracies of sep-tox and normal images at 50% and 85% thresholds displaying performance percentages per class for precision, recall, and accuracy percentage.

Custom Vision Sep-tox Classification Performance Results				
	Threshold (%)	Precision (%)	Recall (%)	AP[1] (%)
Septox	50	100	100	100
Normal	50	100	100	100
Septox	85	100	96.7	100
Normal	85	100	96.3	100

[1]Accuracy Percentage

RStudio Classification. R-Studio was designed to configure a scatterplot using k-means clustering with principal components. Using this unsupervised learning algorithm, RStudio was given only sep-tox images to distinguish if there were significant differences that could be established and help categorize levels of birds that were deemed with this carcass condemnation.

In Figure 2.5, the different clusters are displayed. Cluster 1 had the most images with 252 images, Cluster 2 had 146 images, and cluster 3 had 214 images totaling to 612 images. The scatterplot shown in Figure 2.6 displays the different variations of the cluster sizes. The clusters were very close in proximity, causing an overlap between each cluster. Cluster 1 had the most overlap with Cluster 3 where both clusters contained more images than Cluster 2. Cluster 1 and Cluster 2 had very minimal overlap. Although Cluster 2 and Cluster 3 had some overlap, the overlap was minimal when comparing Cluster 1 and Cluster 3. To get a better concept of each cluster, images from each cluster were selected to see a comparison (Figure 2.7). Cluster 1 and Cluster 3 had the most crossover due to the similarity in appearance. Images from Cluster 1 had the palest skin on the breast when compared to the other clusters. The breast frame size in the images appeared longer and skinnier in size creating an almond-like or "v-like" shape in Cluster 1 being a distinct difference between the other two clusters. As for Cluster 3, the chicken carcasses were paler in color but had more red tone to them on the breast and leg section. The images examined in Cluster 2 had the reddest tone in appearance while the breast size of these birds was similar to Cluster 3, being wider in stature. These different clusters showed variations of color, breast size, and shape of birds that are recognized as sep-tox. By identifying variations of sep-tox, this data can be used to evaluate correlations between bird health and resulting septicemia-toxemia at processing within a flock to better predict future flock needs.

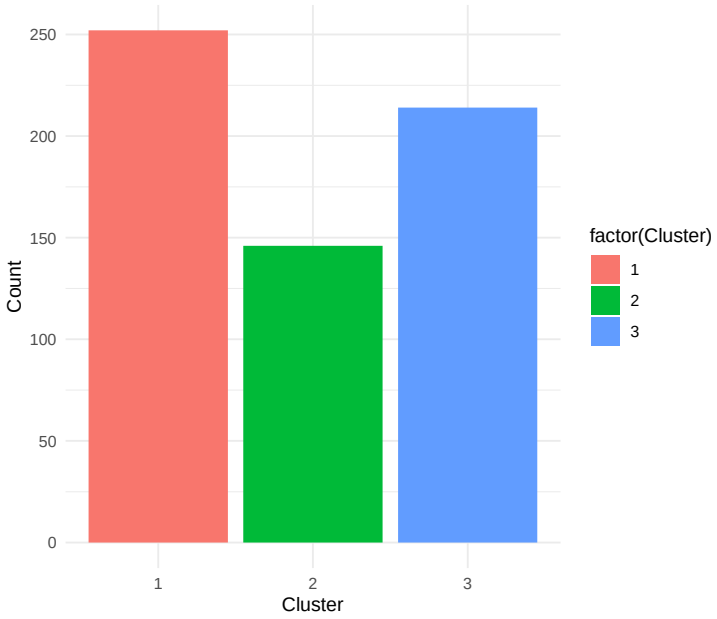

Figure 2.5. Bar graph of sep-tox bird images.

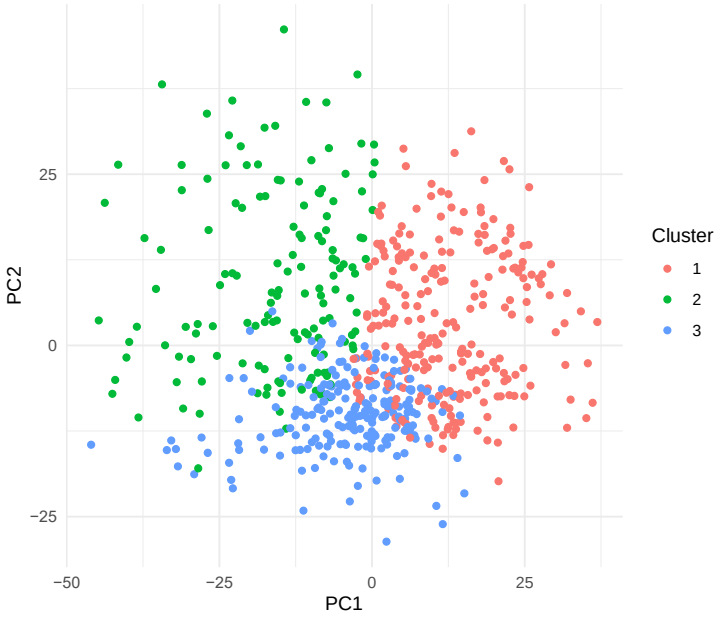

Figure 2.6. Scatterplot of sep-tox bird images.

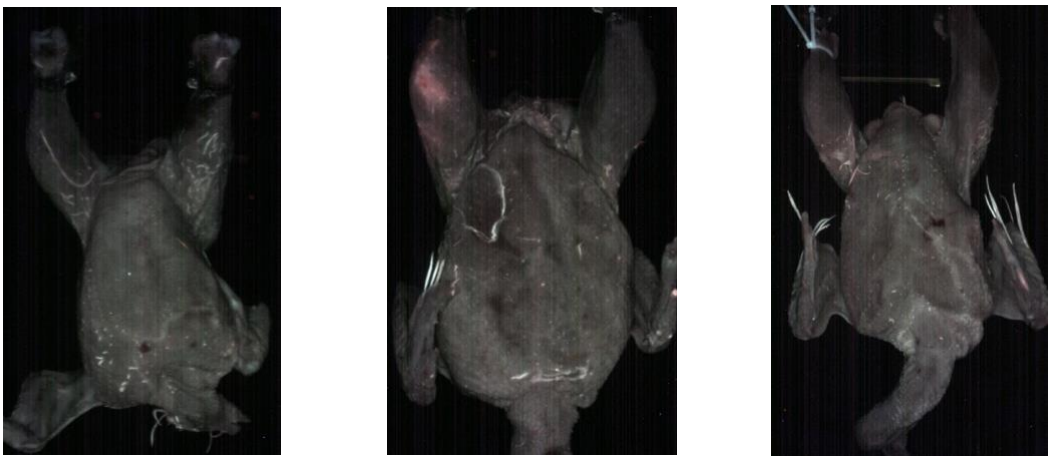

(a) (b) (c)

Figure 2.7. Sep-tox images from Cluster 1 (a), Cluster 2 (b), and Cluster 3 (c) displaying the differences observed in each cluster.

Detection of unwholesome birds using spectroscopy is a method that has been used for almost two decades and has been improved over time by examining whole chicken carcasses for viscera inspection (Chao et al., 1999; Kim et al., 2006). Kim et al. (2006) used fluorescence spectroscopy to determine the characteristic properties of wholesome chicken and chicken visually identified as diseased with air sacculitis, sep-tox, and cadavers by the on-site USDA-FSIS veterinarian. This method used a spectrofluorometer with interactance and reflectance spectra fluorescing the skin of processed birds from their breast for measurement to observe the potential of applying spectroscopy on processing lines for classification of condemned and normal carcasses on intact epidermal skin layers (Kim et al., 2006). To observe these readings when interactance spectra was used, the spectrofluorometer had direct contact with the breast of the chicken carcass. The readings were given by the observation of excitation and emission wavelengths on a matrix compared to an image source produced by the CSI-D+ system. Results concluded in a 97.1% and 94.8% classification between wholesome and unwholesome carcasses. In comparison to the CSI-D+, the spectrofluorometer had direct contact with the carcasses was

required to spot the differences between normal and sep-tox carcasses. Whereas the CSI-D+ did not require direct contact with carcasses for production purposes.

A study using color image classification with a hyperspectral-multispectral line-scan imaging system has been researched for poultry carcass inspection during processing for separating carcasses into unwholesome and wholesome (Chao et al., 2007). Chao et al. (2007) used a suitable region of interest (ROI) on the chicken images where specific wavelengths were required for the classification of infectious birds to assist in configuring 400 masked line-scan images into a hyperspectral image cube of a whole chicken carcass. This allowed the carcass to be examined from any angle to determine if there were any factors that could lead to condemnation located on the carcass. The researchers also detected various oxidative forms of myoglobin, oxymyoglobin, deoxymyoglobin, and metmyoglobin and used them to differentiate between wholesome and diseased birds. This fuzzy method gave a combined classification accuracy of 96% for birds that are deemed systemically diseased (Chao et al., 2007). This study successfully identified wholesome and systemically diseased birds at 100% accuracy at a 40% threshold. When the threshold was increased, the unwholesome carcasses were recognized for rejection but 11% of wholesome carcasses were misclassified for rejection. This study was not able to increase the threshold with 100% accuracy for both classes above 40% compared to the current study where thresholds were held at 50% and 85% without misclassification. Chao et al. (2007) used 55 channels and provided 400 line scan images for completion of a full carcass image. The current study also is ideal for image classification with only using three wavelengths and one image to capture the full carcass in the image.

Overall, spectral imaging was demonstrated to have accurate classification for processed chicken carcasses as wholesome or unwholesome.

Conclusion

Having a technical approach to help with the detection and identification of septicemia-toxemia chicken carcasses was concluded to be successful. Through experimentation, images were able to produce good results with over 95 percent accuracy. However, the first experiment images, sessions 1-4, were too saturated resulting in an image not as clear as expected. With the revision of images and modified camera parameters, clearer images and little to no saturation in the images was achieved. With promising results from the deep learning analytic algorithms, the CSI-D+ camera has potential to help with aiding in the detection of septicemia-toxemia chicken carcasses in processing plants. A limitation of this study is the data extraction from the images to gain intensity values to help predict the differences of carcasses and the need to have a better understanding of set wavelengths used to help identify unwholesome carcasses with the system. Knowing the intensity values from the breast of the chicken carcasses will help determine the variation of birds deemed sep-tox to be more reliable on the principal components demonstrated in RStudio. Although clusters were able to be formed, the clusters were close in proximity. Providing more discernable values will provide a better idea of the severity of sep-tox within these birds. Both CNN models were able to classify all images at 100% accuracy. Using the CSI-D+ system allowed examination of whole chicken carcasses without probing the breast to show differences in wholesome and sep-tox carcasses. The camera is currently handheld, so testing on processing plant lines for real-world evaluation will give more accurate results on how effective the CSI-D+ system could be within a commercial broiler processing facility. Implementing an inspection station for stationary use could improve accuracy and help reduce the workload in the processing plants for trained plant workers who are required to remove condemned birds off the

processing line. Organizing an autonomous system with this easy-to-use and rapid system to differentiate sep-tox birds from normal birds would be beneficial for the NPIS program for real-world applications. With the identification of differences in sep-tox birds through PCA analysis, a model can be configured to distinguish the potential health correlation for each flock.

REFERENCES

Boehmke, B. 2018. Principal Components Analysis. Principal Components Analysis · UC Business Analytics R Programming Guide. https://uc-r.github.io/pca.

Chao, K. 2010. Online inspection. Handbook of Poultry Science and Technology:683–701. ((Chao, K. 2010. "Online Inspection." In I. G. Legarreta and Y. H. Hui, edited by. Handbook of Poultry Science and Technology (Vol. 1). NJ, USA: Primary Processing. John Wiley & Sons; 683–701.))

Chao, K., Y. R. Chen, and D. E. Chan. 2004. A Spectroscopic System for High-Speed Inspection of Poultry Carcasses. Applied Engineering in Agriculture, 20:683–690.

Chao, K., C.-C. Yang, M.S. Kim, and D.E. Chan. 2008. High Throughput Spectral Imaging System for Wholesomeness Inspection of Chicken. Applied Engineering in Agriculture, 24:475–485.

Chao, K., C. C. Yang, Y. R. Chen, M. S. Kim, and D. E. Chan. 2007. Hyperspectral-Multispectral Line-Scan Imaging System for Automated Poultry Carcass Inspection Applications for Food Safety. Poultry Science 86:2450–2460.

Chao, K., Y.R. Chen, H. Early, and B. Park. 1999. Color Image Classification Systems for Poultry Viscera Inspection. Applied Engineering in Agriculture, 15:363–369.

Corporation, NCC. 2024. Light Detection and Ranging (LIDAR). Light Detection and Ranging (LiDAR) System Design Available at https://www.newport.com/n/lidar.

Dey, B.P., Y.R. Chen, C. Hsieh, and D.E. Chan. 2003. Detection of Septicemia in Chicken Livers by Spectroscopy. Poultry Science, 82:199–206.

Kim, M. S., Y. R. Chen, S. Kang, I. Kim, A. M. Lefcourt, and M. Kim. 2006. Fluorescence Characteristics of Wholesome and Unwholesome Chicken Carcasses. Applied Spectroscopy, 60(10):1210–1216. https://doi.org/10.1366/000370206778664644.

Organisation for Economic Co-operation and Development (OECD). 2017. Meat consumption. OECD iLibrary. https://www.oecd-ilibrary.org/agriculture-and-food/meat-consumption/indicator/english_fa290fd0-en.

Sueker, M., K. Stromsodt, H. T. Gorji, F. Vasefi, N. Khan, T. Schmit, R. Varma, N. Mackinnon, S. Sokolov, A. Akhbardeh, B. Liang, J. Qin, D. E. Chan, I. Baek, M. S. Kim, and K. Tavakolian. 2021. Handheld Multispectral Fluorescence Imaging System to Detect and Disinfect Surface Contamination. Sensors 21:7222.

Super, T. 2018, July 24. Survey Shows Us Chicken Consumption Remains Strong. National Chicken Council. Retrieved November 24, 2021, from

https://www.nationalchickencouncil.org/survey-shows-us-chicken-consumption-remains-strong/.

United States Department of Agriculture National Agricultural Statistics Service (USDA-NASS). 2024. USDA Economics, Statistics and Market Information System. Available at https://usda.library.cornell.edu/.

United States Department of Agriculture Food Safety and Inspection Service (USDA-FSIS). 2021. Food Safety and Inspection Service. FSIS Stabilization Guideline for Meat and Poultry Products (Revised Appendix B) | Food Safety and Inspection Service Available at https://www.fsis.usda.gov/guidelines/2021-0013.

United States Department of Agriculture Food Safety and Inspection Service (USDA-FSIS). 2014. "Compliance Guideline for Training Establishment Carcass Sorters in the New Poultry Inspection System (NPIS)." FSIS-GD-2014-0013. https://www.fsis.usda.gov/guidelines/2014-0013.

United States Department of Agriculture Food Safety and Inspection Service (USDA-FSIS). 2022. Broiler Chicken Industry Key Facts 2021. National Chicken Council, Available at https://www.nationalchickencouncil.org/about-the-industry/statistics/broiler-chicken-industry-key-facts/.

Wang, D., F. Tian, S.X.Yang, Z. Zhu, D. Jiang, and B. Cai. 2020. Improved Deep CNN with Parameter Initialization for Data Analysis of Near-Infrared Spectroscopy Sensors. Sensors, 20:874.

CHAPTER III.

Application of Fluorescence Imaging on Chicken Carcasses for the Detection of Visible and Invisible Fecal Contaminations

Abstract
The USDA-FSIS implements a zero visible fecal tolerance policy on WOGs entering into the chiller in efforts to enhance food safety. With the introduction of the New Poultry Inspection System, plant personnel undergo training to identify carcass condemnations, including fecal contamination. A study was conducted to assess the efficacy of spectral imaging technology in detecting visible fecal matter, aiming to enhance automation in processing plants. Additionally, the investigation explored the capability of the imaging system to identify fecal contamination even after WOGs undergo reworking (washing), highlighting the potential risk of invisible (to the human eye) fecal matter as a source of Salmonella contamination. Eviscerated broiler carcasses (weighing 8-10lbs live weight) were collected from a processing plant. Fecal contamination from the ceca (~100g) was collected and inoculated with an 18-hour *Salmonella* Typhimurium culture, which was then applied to the breast skin of the chicken carcasses for examination. Inoculated carcasses (n=100) were suspended by shackle in a light-free enclosure and scanned using a handheld spectral imaging system. Images were captured before inoculation, after inoculation, and after spraying the fecal-contaminated area of the carcasses with water. Subsequent image analysis was conducted using Microsoft Custom Vision. Carcasses were swabbed after each imaging session and subjected to a 24-hour incubation in Brain Heart Infusion (BHI) broth for BioMerieux GeneUp *Salmonella* PCR assay testing. The imaging revealed that fecal contamination could indeed be identified using the spectral camera. Furthermore, image analysis indicated the presence of fecal remnants, invisible to the human eye, on the WOGs. *Salmonella* analysis of all 100 WOGs prior to fecal contamination yielded negative results for the pathogen. However, *Salmonella* was detected in those areas following the reworking of the carcasses to eliminate fecal matter. Custom Vision classification results demonstrated 100% precision and 83.3% recall, resulting in a 99.4% accuracy rate. The findings

of fecal matter invisible to the human eye underscores the necessity to enhance reworking procedures and develop improved protocols for thoroughly eliminating all traces of fecal contamination to lower food safety risks.

Introduction

With over 9 billion broiler chickens being produced yearly in the United States, the poultry industry is the largest meat producing industry in the world. The poultry industry has grown tremendously in the United States the last 40 years, with broiler chicken consumption doubling from 48.8 pounds in 1984 and now reaching 98.9 pounds of broiler chicken being consumed per capita in 2022 (NCC Admin & USDA, 2022). Satisfying the rising demand necessitates an increase in poultry production, with equal importance given to ensure poultry meat safety at different stages of poultry meat production including processing plants. One of the traditional food safety steps in poultry processing plants is the inspection of poultry carcasses for carcass wholesomeness implemented under the Poultry Product Inspection Act of 1957. Further, the introduction of the voluntary New Poultry Inspection System (NPIS) in 2014 allowed trained plant personnel to inspect carcasses and allowing USDA-FSIS to focus on food safety activities (Chowdhury and Morey, 2020). The inspection involves U.S. Department of Agriculture-Food Safety and Inspection Service (USDA-FSIS) inspectors or trained plant personnel to be placed on the processing line to investigate carcasses and viscera visually and physically for factors such as fecal contamination, diseases, or defects. The presence of fecal matter increases *Salmonella* and *Campylobacter* food safety risks of raw poultry and hence it is important that carcasses with fecal contamination be accurately detected and reworked. However, visual inspection and detection of fecal contamination on fast moving poultry processing lines allows an inspection time of 35 birds per minute (Dey et al., 2003; Yoon et al., 2011). Such high speeds

may introduce human error in detecting fecal contamination and increase food safety risks of raw poultry. It is imperative that rapid technologies to detect fecal matter on carcasses should be evaluated to reduce the spread of contamination and improve food safety.

With the use of an automated system that can target carcass condemnations and reduce repetitive work actions during inspection would be beneficial to the industry's inspection system.

In recent decades, spectral imaging has become more prominent in the industry, proving itself to be beneficial for inspection purposes. Chen and Massie (1993) utilized a visible/near-infrared reflectance spectroscopy system to identify unwholesome birds that were either had sep-tox conditions or cadavers deemed by veterinarians. Park et al. (2005) observed cecal contaminants using spectral imaging on broiler carcasses in the visceral cavity with a classification accuracy ranging from 75.9% to 96.69%. A constant issue for the algorithms was the missed contaminants or false positives depending on the median filter that was applied at each set threshold value. Other limitations to this study were only cecal material was used without the addition of other contaminants that could be present during processing and half birds were used, whereas, in processing plants, whole birds are evaluated for contamination. Fecal contamination is not only a problem for consumed products but can also be found on equipment surface which creates an unclean environment for processing plants. Organic material and fecal contamination primarily remain on processing equipment during processing.

Scientists have observed processing equipment with fecal matter and ingesta contamination using reflectance and interactance light to detect organic residues and ingesta based off of intensity changes based on different wavelengths on stainless steel (Park et al., 2005; Qin et al., 2011). Fluorescence light is a highly sensitive method, capable of detecting even the most subtle changes in biological material such as animal tissues (Qin et al., 2011). Fluorescence

light detection measures the light being emitted from the biological samples excited by high-intensity UV-B or narrowband light (Qin et al., 2011). On the other hand, LED lights have an advantage compared to other lights due to their longevity, low heat, response time, and consumption of power source. A study was conducted using fluorescence techniques to assist with safety inspection using light emitting diode (LED) excitation line-scanning imaging system on stainless steel to detect chicken fat, blood, and fecal matter (Qin et al., 2011). Principal components analysis (PCA), an unsupervised data analysis method, was used for data analysis models for classification and identify key wavelengths. The researchers found that excitation wavelength for fecal matter, fat and blood were 580 nm, 570-610 nm and 618 nm, respectively and formed distinct groups on PCA plots. Among the fecal sources of fecal matter, cecal matter had a distinct spectra and a group while the other sources (duodenum, colon, and small intestine) were difficult to distinguish from each other, resulting in a larger group for these three feces. Seo and team (2019) used a multispectral line-scan imaging system to identify fecal contaminants from the ceca, duodenum, colon, and small intestine at different line speeds (1, 3 and 5 bird per second birds per second). UV lamps were used in addition to the spectral camera for fluorescence. The imaging technology had a 97.5% accuracy for the detection and isolation of the fecal spots for different processing speeds indicating its potential application in a high-speed poultry processing environment (Seo et al., 2019).

A previous study addressed fecal contamination on meat carcasses using a handheld fluorescence imaging system that includes UV settings. Gorji et al. (2022) used raw skinned cattle and sheep carcasses for video recording with, and later without, guidance from a meat inspector for further review of the meat carcasses. In this study, video frames with fecal contamination on meat surfaces and identified segmented areas were evaluated to produce

successful classification of clean and unclean carcass images with the CSI-D system. Gorji et al. (2022) emphasized a need to overcome oversaturation from bright ambient light concerns when fluorescence imaging is used. With the CSI-D system, Gorji et al. (2022) successfully mitigated concerns with difficult visual inspections on meat carcasses in meat processing plants. This handheld system being implemented in processing plants can be the assistance meat processing plants need for the reduction of contaminated samples limiting the spread of foodborne pathogens to consumers.

The current study used a hand-held, multispectral fluorescence system with the following objectives:

(1) Distinguish differences between fecal contaminants from four regions of the gastrointestinal tract.

(2) Detect fecal contamination invisible to the naked eye and establish the presence or absence of *Salmonella* after rinsing.

Materials and Methods

Multispectral Imaging System.

The optical imaging system called Contamination, Sanitation, Inspection, and Disinfection (CSI-D+) system (SafetySpect, Grand Forks, ND) was used for the study. The multispectral RGB images were captured through fluorescence of the camera to illuminate contamination sights on the chicken carcasses. This system was controlled through a wireless connection to a tablet placed within 6 feet of the camera taking still images in .png format at 1024 x 768 pixels where camera parameters that were set are shown in table 3.1. Light Detection and Ranging (LIDAR) was used for measuring the distance between the CSI-D+ device and the carcass surface that was being examined. The LED light cannot be altered and was set at 405nm. Exposure exposed the

photo-sensitive cells to light at 230 and 270 (ms). Gain controlled noise levels in background of images activity set at 1,000 mB, Brightness set at 3 added whiteness to images. Saturation set at 45 created monochrome images. Hue was set at 0 and gamma set at 80. The red and blue balance (RB balance) were both set to 4,000.

Table 3.1. Settings used for CSI-D+ imaging system to fluoresce in ambient light-free conditions.

Camera Settings								
LED (nm)	Exposure (ms)	Gain (mB)	Brightness	Saturation	Hue	Gamma	Red Balance	Blue Balance
405	230; 270	1000mB	3	45	0	80	4000	4000

Detection of fecal matter from different regions of the GI tract.

Freshly slaughtered and chilled whole chicken without giblets (WOGs) weighing 8-10lbs. live weight and gastrointestinal (GI) tracts were collected from a local USDA-inspected commercial poultry processing plant and transported to the department of Poultry Science at Auburn University under refrigeration conditions (4 ºC). The GI tracts were examined for abnormalities and dissected to retrieve the fecal contaminants used in this experiment. Fecal matter and digesta (20-25 g each) were collected from the proventriculus, small intestine, large intestine, and ceca. A polypropylene stamp (0.8 cm and 2.5 cm dia) was used to inoculate the contaminants on the breast skin of WOG. The stamp created a small and large sized application point for imaging. Samples were photographed using the multispectral CSI-D+ system in an ambient-light free box placed 12 inches (30.48cm) away from the chicken carcass that is hung by a processing plant shackle for a more controlled background setting in this study. Each contaminant with small and large applications points were placed on a different carcass to not interfere with fluorescence. This process was reproduced for six sessions that produced 50

images on average of each contaminant for every exposure time and application size. A total of 404 birds were used with 1,614 images composed.

Detection of fecal contamination invisible to the naked eye and occurrence of Salmonella.

In a separate experiment, post-chill chicken WOGs and GI tracts were collected as stated above. Cecal matter from the ceca (100 g) was collected and inoculated with an 18-hour grown culture of *Salmonella* Typhimurium (35µg nalidixic acid resistant) to obtain a final concentration of 10^5 CFU/g which was plated out using the selective media, Xylose Lysine Deoxycholate (XLD) agar, for validation. Prior to the inoculating cecal matter, each WOG was imaged twice using the CSI-D+ at 230 and 270 ms exposure (Table 3.1) to ensure absence of fecal contamination. After imaging, the carcass was removed and swabbed with a sterile foam swab tip (2.5 x 2.5 cm) on the crown of the skin-on breast (region of interest; ROI) and placed into 9mL Brain Heart Infusion (BHI) broth to be analyzed using the GeneUp® PCR-based procedure (described below) for presence of *Salmonella* spp.

Further, the polypropylene rubber stamp (2.5 cm dia.) was used to inoculate the *Salmonella* contaminated cecal remnants on the ROI and then placed into the box for imaging. After imaging with inoculation, the ROI was swabbed again and later analyzed using the procedure described below. To mimic processing plant methods, the inoculated WOGs were sprayed with deionized water (DI) water using a water bottle to remove visible contamination with 50 sprays and images were taken as per the standard protocol followed by swabbing of the ROI. A total of 100 chicken carcasses over five trials were used producing 600 images (3 images per carcass x two exposure times) and 300 swabs were incubated for PCR assay testing for laboratory settings.

In-plant validation of the CSI-D+ and presence of Salmonella.

An additional three sessions were conducted where equipment was taken and set up at the commercial processing plant and utilized in a similar fashion as the laboratory setting. Eviscerated carcasses spotted with fecal contamination by trained plant workers and were removed from the processing line for fluorescent imaging (CSI-D+). Contaminated carcasses were rinsed off with an antimicrobial agent by the trained worker and imaged again. Each contaminated carcass was swabbed before and after rinsing for further analysis of *Salmonella* presence using the GeneUp PCR Assay. A total of 57 carcasses were collected from these sessions resulting in 225 images taken and 114 swab samples for prevalence.

PCR Assay.

In total, 414 swabbed samples, from the laboratory and in-plant studies, were analyzed for the presence of *Salmonella* spp. Swabs from each sampling in BHI broth test tubes were enriched at 37ºC for 24h and further analyzed on BioMerieux (MO) GeneUp PCR Assay for the probable presence or absence of *Salmonella* spp. (bioMerieux, 2020). Additionally, a positive and negative control were prepared for testing. The transferring of twenty microliters (µL) of the incubated samples were pipetted into lysis tubes. The lysis tube plate was vortex for five minutes at 2200 rpm. Lysed samples are removed and prepared for transfer to PCR tubes. The lysed samples were pipetted 10 µl into *Salmonella* PCR assay tubes and spun down for ten seconds to remove any excess liquid from the optical caps. PCR tubes are placed into the GeneUp and ran for analysis. GeneUp analysis was ran for less than an hour to produce presumptive positive or negative samples of *Salmonella*.

Image Classification.

Google Collaboration Convolution Neural Network. Convolution neural network (CNN) deep-learning model was utilized in this study. Derived from the Artificial Neural Network (ANN) system, the CNN model is employed for image classification, segmentation, and achieving high performance and accuracy in object recognition (Ramdani et al., 2020; Ristiawanto et al., 2019). Specifically, the CNN model is employed for image classification within a food detection system, particularly in dining environments, due to its advanced knowledge representation capabilities. (Ramdani et al., 2020). Image analysis was performed using the Convolution Neural Network (CNN) algorithm on Google Collaboratory with Adam Optimizer using 50 epochs at a learning rate (lr) of 0.001 and weight decay (wd) value of 0.0001. The process of working with the CNN model involves three main steps: image uploading and sorting, model configuration, and validation. Image classification of contaminant variation was ceca versus large intestine versus proventriculus versus small intestine after uploading images into their respective folders. Additionally, image augmentation techniques were applied to enhance the robustness of the model. Data augmentation types consisted of the following: image size reduction (150 L x150 W), a vertical and horizontal flip, and a random rotation. Image classification was performed using 70::30 ratio. The images were places in three separate folders where the 70% of images were used for training the model, 20% of the images were used for testing the model which would select the best testing model for the validation step. Subsequently, a validation test was conducted using a subset of images to ensure the accuracy of the model with the last 10% of the images. The best model was selected based on its accuracy and loss tensor, which was indicative of the model's classification accuracy. The best generated test model saved for validation which was created after 50 epochs or iterations with a lr of 0.001 and

wd of 0.0001. In the final validation step, the selected model was applied to an unidentified set of images to categorize them into their respective four different categories. An image analysis model was created for further image analysis using platform CUDA 11.2 and Pytorch machine learning framework with three ConvNet layers.

Custom Vision. Custom Vision, leveraging the Microsoft Azure platform, was operated. This system utilizes machine learning techniques through a CNN algorithm to train a custom multi-class image classification model in real-time. Post-training, performance metrics such as precision, recall, and accuracy percentage are evaluated to assess the model's classification accuracy. The threshold for probability scoring can be adjusted to optimize the model's performance during image classification was set at 50%. Four different models were made for the two exposure times, 230 and 270 ms, and the various fecal matter sizes administered onto the chicken carcasses for the first objective and used both CNN algorithm platforms. The second objective of this study depended solely on Custom Vision for the image analysis system with three models created.

Results and Discussion

Fluorescence imaging.

Fluorescence imaging using CSI-D+ was able to detect fecal contamination (Figures 3.1 and 3.2) irrespective of the exposure times (230 and 270 ms) and the size of contaminant (0.8 and 2.5 cm). Images of contaminants from different GI tract regions had some distinct differences. Digestion of the ingested feed is initiated in the proventriculus through the introduction of enzymes and gastric juices and then it gets digested, and the proteins are absorbed in the small intestine (Jacob, 2024). The ceca, two elongated pouches, interconnect the small and large intestines where some water absorption and fermentation occur for the digested

feed (Jacob, 2024). Lastly, the large intestine is where final water reabsorption of the digested material takes place before exiting the chicken through the cloaca (Jacob, 2024). The different consistencies of contaminants are relative to the stages the feed is in the digestive system. Ceca samples had a smooth appearance with a darker tone of red and had a firm, thick consistency to it while small intestine samples had a deeper tone of red and a looser, chunky consistency and in some images was running down the chicken carcass when changing exposure times. The large intestine samples had a pale redness to the contaminant where the consistency was thinner when compared to the proventriculus samples that had a brighter red tone color with a clumpier, feed-like consistency.

Fecal matter from poultry, in recent studies, can possibly include blood substances such as myoglobin. Myoglobin is an iron ion responsible for carrying oxygen and giving meat its color (Courrol & Samad, 2018). An organic group found in myoglobin, called porphyrins, contain a subgroup, known as protoporphyrin IX, that accumulates in meat products at production time exhibits fluorescence (Courrol & Samad, 2018; Seo et al., 2019). Porphyrin can also be produced by different microorganisms at increased temperature and atmospheric conditions exciting at 420nm and fluorescing from 500 to 750 nm (Silva et al., 2012; Courrol & Samad, 2018). This protein is likely found in fecal matter giving contribution to fluorescence of this matter given excitation of protoporphyrin IX and chlorophyll, another constituent known for fluorescence, found in undigested feed material during digestion (Chao et al., 2008; Courrol & Samad, 2018).

Cecal contamination was used for the second objective due to the importance it brings to the digestive system and health of the bird. The ceca have an important role of fermenting of remaining digested material for continuance of breaking down undigested material, the transport

for electrolytes, and water absorption for the chicken. Observations from Objective one indicates, the cecal content displayed a deep red color when placed on the breast skin of the chicken carcass. Images taken before inoculation, showed no sign of fecal contamination upon receiving. The inoculated carcass successfully shown where cecal matter had been placed on the breast. Once the carcass was rinsed with DI water, the presence of fecal contamination could not be seen with the naked human eye, but a white spot emitted when fluorescence images were taken. This spot was apparent on every carcass that was inoculated signifying where the cecal matter was placed previously upon rinsing.

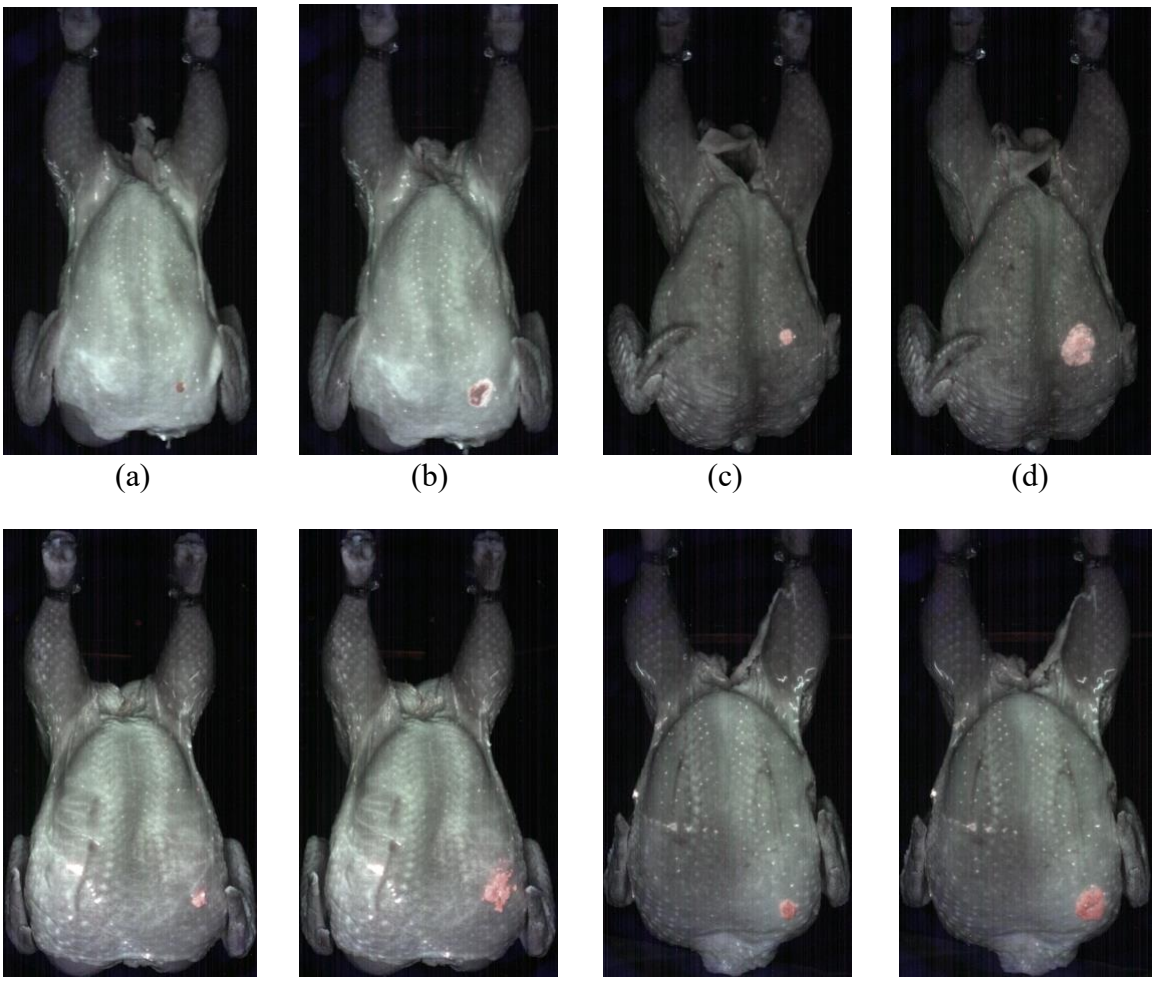

Figure 3.1. Images of chicken carcass at with fecal matter of (a-b) ceca, (c-d) large intestine, (e-f) proventriculus, and (g-h) small intestine with both small and large applications of rubber stamp at 230ms exposure.

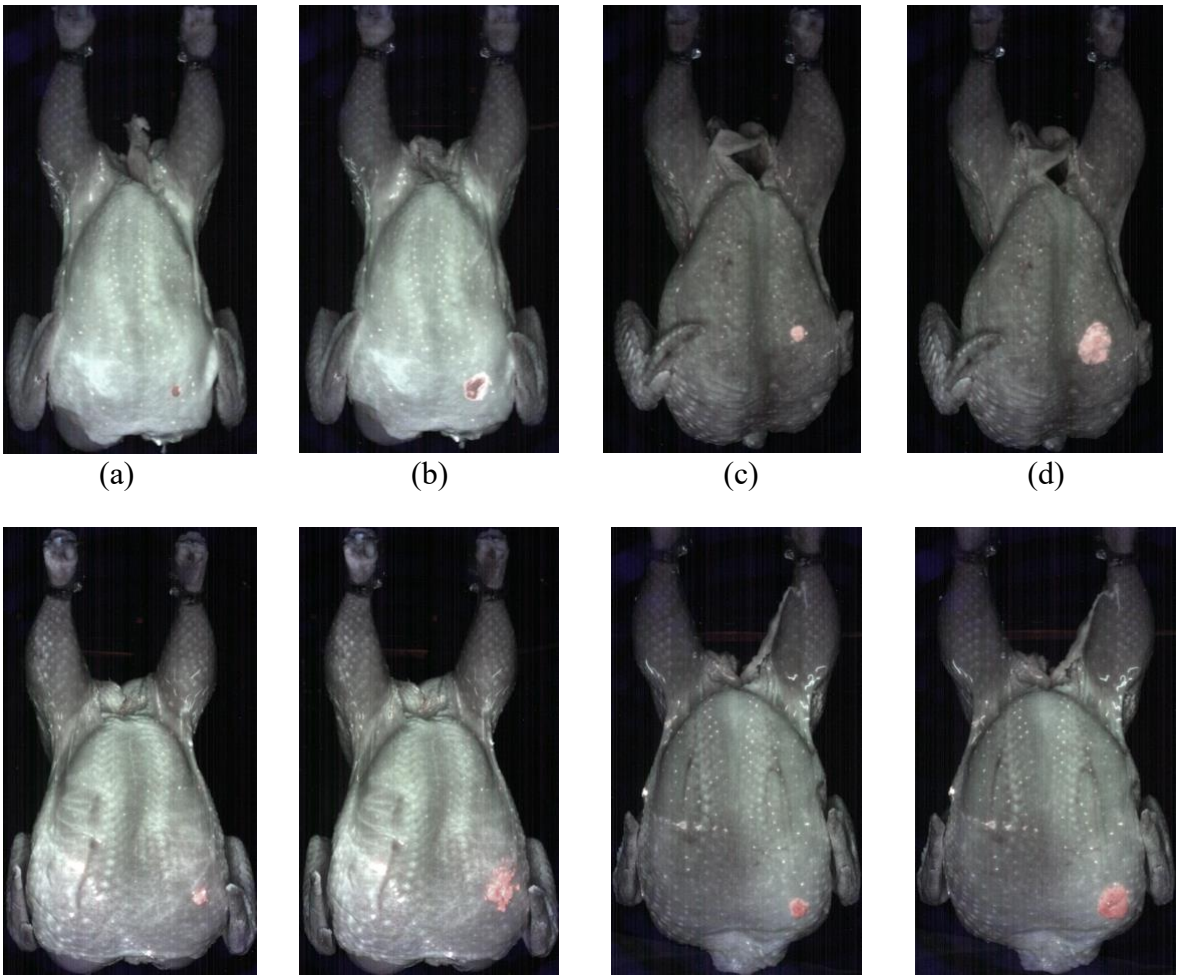

(a) (b) (c) (d)

(e) (f) (g) (h)

Figure 3.2. Images of chicken carcass at with fecal matter of (a-b) ceca, (c-d) large intestine, (e-f) proventriculus, and (g-h) small intestine with both small and large applications of rubber stamp at 270ms exposure.

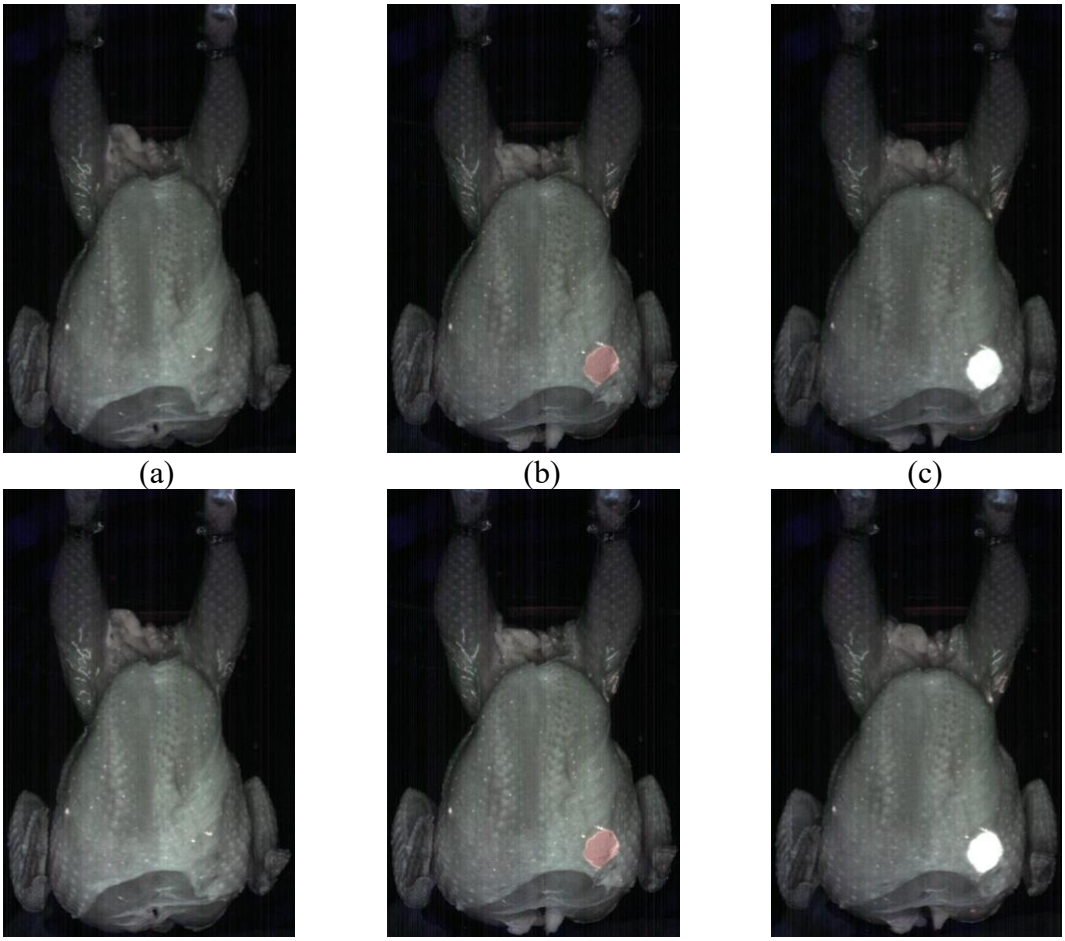

Figure 3.3. Images of chicken carcass before inoculation of fecal matter, with inoculation of fecal matter, and after rinsed with deionized water at exposure times of (a-c) 230ms and (d-f) 270ms.

Classification model performance for different contaminants.

Four models were built for classification of the different fecal contaminants and digesta using Google Collaboration. The classification models were carried out with an average of 200 frames per model where inoculated carcasses were used in Table 3.2 listing the standard deviation and average for each exposure time and contaminant size. The model was trained with a 70::30 split for each model where 70% of images went to the training set, 20% for validation of the model, and 10% of the images used for evaluation of the model performance; these images were all selected at random for these folders. As shown in Table 3.2, the contaminants were able to be classified into their own category at various accuracy percentages. The contaminant,

proventriculus, had the best outcome across all four models while the large intestine sample had the least percentage accuracy. Proventriculus had the highest percent accuracy at 49.93% for the small application size at 230ms exposure. Small intestine was classified with a 47.60% accuracy while ceca had a 40.08% accuracy for the large application size at 270ms exposure. The remaining percent accuracies were relatively low. A second CNN algorithmic platform was used for comparison of platform performances. Custom Vision resulted in having a better percentage accuracy in some classifications when threshold was held at 50 in Tables 3.3 and 3.4. The large intestine sample was able to increase the accuracy from 0.002% to 39.10% accuracy rate when large application point at 270ms exposure when compared to the other platform. In other cases, Ceca samples reduced in classification from 40.08% to 28.20% when large application at 270ms exposure were compared. Overall, this system concluded better classification results when compared to the program on Google Collaboration. Seo (2019) performed a similar project comparing four contaminants on chicken carcasses. However, this research was classified by detection of fecal matter using color analysis where these contaminants fell on the RGB spectrum that ranged from 430-690nm. Classifying the fecal spots placed on the chicken carcasses resulted in two contaminants, from the ceca and colon, placed into the upper ROI while the other two, small intestine and duodenum, were placed into the bottom ROI and a skin ROI where no fecal matter was placed. The goal for this research was not to identify the fecal matter for all contaminations but to distinguish a difference between the pair of contamination spots placed on the carcass. Three out of the four contaminants used in Seo's project were the same for the objectives of this research, however, the comparison of contaminants amongst each other were not a part of the objective described in their research. Complications with these models

involved fluorescence of feather follicles on some carcasses which led to misclassification.

Another limitation to misclassification is the minute data set for each model program built.

Table 3.2. Summation of percentage accuracy average and standard deviation for classification between fecal contaminants exposure time and contaminant size from CNN model performed in Google Collaboration.

Fecal Matter Percentage Accuracy (%) Validation Results					
Application Size	**Exposure time**	**Ceca**	**Large Intestine**	**Proventriculus**	**Small Intestine**
Large	**230 ms**	17.592 ± 19.138	34.495 ± 12.755	29.893 ± 16.583	8.667 ± 7.978
Large	**270 ms**	40.084 ± 43.508	0.002 ± 0.004	16.408 ± 18.025	47.596 ± 34.345
Small	**230 ms**	11.431 ± 10.425	15.426 ± 4.783	49.928 ± 22.540	17.660 ± 12.570
Small	**270 ms**	42.819 ± 24.097	9.826 ± 4.926	10.005 ± 6.024	24.197 ± 14.666

Table 3.3. Individual percentage accuracy for classification of fecal matter contaminants sizes and exposure times from Azure Custom Vision displaying accuracy percentage (AP) with threshold.

Fecal Matter Percentage Accuracy (%) Validation Results					
Image Type	**Threshold**	**Ceca**	**Large Intestine**	**Proventriculus**	**Small Intestine**
Large 230 ms	50	46.20	37.80	62.80	57.80
Large 270 ms	50	28.20	39.10	59.10	54.00
Small 230 ms	50	32.50	39.90	52.00	59.50
Small 270 ms	50	37.70	28.10	53.00	33.40

Table 3.4. Overall percentage accuracy for classification of fecal matter contaminants sizes and exposure times from Azure Custom Vision displaying precision, recall, and accuracy percentage (AP) with threshold.

Fecal Matter Performance Percentage Accuracy (%) Results				
Image Type	**Threshold**	**Precision**	**Recall**	**AP**
Large 230 ms	50	66.70	7.10	55.40
Large 270 ms	50	50.00	2.50	41.80
Small 230 ms	50	100.00	7.10	42.10
Small 270 ms	50	60.00	7.50	35.90

Classification model performance for invisible contamination.

The three classes were created for this data set containing 300 images per model. Two models were created from the different exposure times for image analysis using Custom Vision shown in Table 3.5. There were promising results for classification with an accuracy percentage of 99.40% for images taken at 230ms exposure with 50 as the threshold. Since the results at threshold for 50 were promising, threshold was increased to 85 for more accuracy of the platform. When threshold was held at 85, the rate of 99.40% accuracy was concluded with only one image being tagged at 62.90% probability in the right class falling below the set threshold. When exposure time at 270ms was analyzed, both threshold points resulted in 97.20% accuracy rate. An overall percentage accuracy model was created with the images taken at the plant site in table 10 showing precision, recall, and accuracy percentage results. The exposure times were combined together to determine if there was a difference in analysis when combined. The model showed when threshold was held at 50 and 85 a result of 97.80% accuracy rate. The prediction model can be an advantage to the development of automated system approaches in the poultry industry.

Table 3.5. Percentage accuracy for classification of fecal contamination exposure times before inoculation, during inoculation, and rinsed samples from Azure Custom Vision displaying precision, recall, and accuracy percentage (AP) at two thresholds.

Custom Vision Prediction Percentage Accuracy (%) Results				
Exposure Time (ms)	**Threshold**	**Precision**	**Recall**	**AP**
230	50	96.60	95.00	99.40
230	85	100.00	80.00	99.40
270	50	93.30	93.30	97.20
270	85	100.00	40.00	97.20

Table 3.6. Percentage accuracy of overall images before inoculation, during inoculation, and rinsed samples from Azure Custom Vision displaying precision, recall, and accuracy percentage (AP) at two thresholds.

Custom Vision Prediction Percentage Accuracy (%) Results			
Threshold	**Precision**	**Recall**	**AP**
50	93.80	92.10	97.80
85	99.10	63.60	97.80

Salmonella PCR assay.

Samples from the laboratory setting are discussed in Table 3.7 where only 60 test samples were recovered due to technical issues with the PCR device. From the 60 samples, 58.33% of these samples were found negative before inoculation of the cecal matter. These 35 samples were looked into further of their results after inoculation and after rinsing. After further review, 97.14% of the samples that were initially negative transpired to positive samples once inoculated and rinsed with DI water. Rinsing the cecal matter until not visible was not successful in removing the presence of *Salmonella*. Samples found contaminated in plant settings, were 9.65%. With the use of microbial agents for rinsing of contaminated carcasses in plant settings out of the 11 samples, 27.27% of these samples were found positive after antimicrobial rinsing of the carcass (Table 3.8). This information is beneficial on moving forward with the protection of poultry carcasses in the food industry. The presence of *Salmonella* is possible due to the antimicrobial resistant microorganism attachment onto the skin of the chicken carcass.

Table 3.7. Swabbed samples from before inoculation, during inoculation, and after rinsing of fecal contamination for the presence or absence of *Salmonella* spp. using GeneUp® PCR machine.

BioMerieux GeneUp® *Salmonella* PCR Assay Results						
	Before Inoculation		**Inoculated**		**After Rinsing**	
Salmonella Detected	Positive	Negative	Positive	Negative	Positive	Negative
Samples no. Tested	25	35	34	1	34	1
Percentage (%)	41.67	58.33	97.14	2.86	97.14	2.86

Table 3.8. Plant setting swabbed samples from contaminated and after rinsing of fecal contamination for the presence or absence of *Salmonella* spp. using GeneUp® PCR machine.

BioMerieux GeneUp® *Salmonella* PCR Assay Results				
	Contaminated		**After Rinsing**	
Salmonella Detected	Positive	Negative	Positive	Negative
Samples no. Tested	11	103	3	8
Percentage (%)	9.65	90.35	27.27	72.73

Conclusion

In this work, a handheld multispectral fluorescence imaging system for detection of various fecal contaminants and invisible fecal contamination using based on CNN image analysis algorithms was successful. The findings in this research indicates that the direction of spectral imaging systems in poultry processing plants is beneficial to the poultry industry. When determining the difference detection of the contaminants from ceca, large intestine, proventriculus, and small intestine, it is important to know the origin of contamination. The knowledge of contamination origin can allow the adjustment of evisceration equipment to reduce cutting these organs. Creating a larger data set for each contaminant size and exposure time will allow the models' performance to increase the accuracy percentages given datasets gathered were comparably small to other studies. With a minimal amount of data being gathered, the model performances were not able to produce higher differential classifications. Given the limited

amount of data, retrieving 49.93 and 55.40% accuracy rates in classification is promising work. Training these models with more data will be most beneficial for future studies. The second objective on invisible fecal matter showed promising results achieving a 97.80 to 99.40% accuracy rate for classification when compared to chicken carcasses that had visible contamination and no contamination found on the carcass. In regard to rinsing with DI water and recovering *Salmonella*, this exhibits a potential indication source on foodborne pathogens contacting consumers. To further develop this inspection system, additional research with an antimicrobial agent is necessary to determine the presence of *Salmonella* after fecal contamination has been rinsed from the contaminated carcass. Further research needs to be conducted on contaminated samples at poultry processing sites to create a stronger awareness of invisible fecal matter on rinsed carcasses.

REFERENCES

bioMerieux, Inc (bioMerieux). 2020. GENE-UP® *Salmonella* (SLM2)GENE-UP® *Salmonella* (SLM2) All human food products & production environmental samples. GENE-UP® *Salmonella* (SLM2) Available at https://www.biomerieux-usa.com/sites/subsidiary_us/files/us_gene-up_salmo-quickguide.pdf (verified 3 March 2024).

Chao, K. 2010. Online inspection. Handbook of Poultry Science and Technology:683–701. ((Chao, K. 2010. "Online Inspection." In I. G. Legarreta and Y. H. Hui, edited by. Handbook of Poultry Science and Technology (Vol. 1). NJ, USA: Primary Processing. John Wiley & Sons; 683–701.))

Chao, K., Y. R. Chen, and D. E. Chan. 2004. A Spectroscopic System for High-Speed Inspection of Poultry Carcasses. Applied Engineering in Agriculture, 20:683–690.

Chao, K., X. Nou, Y. Liu, M. S. Kim, D. E. Chan, C.-C. Yang, J. Patel, and M. Sharma. 2008. Detection of Fecal/Ingesta Contaminants on Poultry Processing Equipment Surfaces by Visible and Near-Infrared Reflectance Spectroscopy. Applied Engineering in Agriculture 24:49–55.

Chen, Y. R., and D. R. Massie. 1993. Visible/Near-Infrared Reflectance and Interactance Spectroscopy for Detection of Abnormal Poultry Carcasses. Transactions of the ASAE 36:863–869.

Chowdhury, E. U., and A. Morey. 2020. Application of Optical Technologies in the US Poultry Slaughter Facilities for the Detection Of Poultry Carcase Condemnation. British Poultry Science 61:646–652.

Courrol, L. C., and R. E. Samad. 2018. Determination of Chicken Meat Contamination by Porphyrin Fluorescence. Journal of Luminescence 199:67–70.

Dey, B. P., Y. R. Chen, C. Hsieh, and D. E. Chan. 2003. Detection of Septicemia in Chicken Livers by Spectroscopy. Poultry Science 82:199–206.

Gorji, H. T., S. M. Shahabi, A. Sharma, L. Q. Tande, K. Husarik, J. Qin, D. E. Chan, I. Baek, M. S. Kim, N. MacKinnon, J. Morrow, S. Sokolov, A. Akhbardeh, F. Vasefi, and K. Tavakolian. 2022. Combining Deep Learning and Fluorescence Imaging to Automatically Identify Fecal Contamination on Meat Carcasses. Scientific Reports 12.

Jacob, J. 2024. Avian Digestive System. Small and Backyard poultry Available at https://poultry.extension.org/articles/poultry-anatomy/avian-digestive-system/ (verified 16 March 2024).

Lawrence, K. C., B. Park, W. R. Windham, and C. Mao. 2003. Calibration of a Pushbroom Hyperspectral Imaging System for Agricultural Inspection. Transactions of the ASAE 46.

NCCAdmin and USDA. 2022. Chicken Processors Redoubling Efforts to Keep Essential Workers Safe and Healthy. National Chicken Council Available at https://www.nationalchickencouncil.org/chicken-processors-redoubling-efforts-to-keep-essential-workers-safe-and-healthy/ (verified 16 March 2024).

Park, B., K. C. Lawrence, W. R. Windham, and D. P. Smith. 2005. Detection of Cecal Contaminants in Visceral Cavity of Broiler Carcasses using Hyperspectral Imaging. Applied Engineering in Agriculture 21:627–635.

Qin, J., K. Chao, M. S. Kim, S. Kang, B.-K. Cho, and W. Jun. 2011. Detection of Organic Residues on Poultry Processing Equipment Surfaces by LED-Induced Fluorescence Imaging. Applied Engineering in Agriculture 27:153–161.

Ramdani, A., A. Virgono, and C. Setianingsih. 2020. Food Detection with Image Processing using Convolutional Neural Network (CNN) Method. 2020 IEEE International Conference on Industry 4.0, Artificial Intelligence, and Communications Technology (IAICT).

Ristiawanto, V., B. Irawan, and C. Setianingsih. 2019. Wood Classification with Transfer Learning Method and Bottleneck Features. 2019 International Conference on Information and Communications Technology (ICOIACT).

Seo, Y., H. Lee, C. Mo, M. S. Kim, I. Baek, J. Lee, and B.-K. Cho. 2019. Multispectral fluorescence imaging technique for on-line inspection of fecal residues on poultry carcasses. Sensors 19:3483.

Silva, F. R., C. T. Nabeshima, M. H. Bellini, N. Schor, N. D. Vieira, and L. C. Courrol. 2012. Study of Protoporphyrin IX Elimination by Body Excreta: A New Noninvasive Cancer Diagnostic Method. Journal of Fluorescence 23:131–135.

U.S. Department of Agriculture–Food Safety and Inspection Service (USDA-FSIS). 2014. Food Safety and Inspection Service. FSIS Guideline for Training Establishment Carcass Sorters in the New Poultry Inspection System (NPIS) | Food Safety and Inspection Service Available at https://www.fsis.usda.gov/guidelines/2014-0013 (verified 16 December 2023).

Wang, Tian, Yang, Zhu, Jiang, and Cai. 2020b. Improved deep CNN with parameter initialization for data analysis of near-infrared spectroscopy sensors. Sensors 20:874.

Yoon, S. C., B. Park, K. C. Lawrence, W. R. Windham, and G. W. Heitschmidt. 2011. Line-Scan Hyperspectral Imaging System for Real-Time Inspection of Poultry Carcasses with Fecal Material and Ingesta. Computers and Electronics in Agriculture 79:159–168.

SUMMARY

The objective of the research was to identify and differentiate normal broilers and broilers with septicemia-toxemia (septox) using a handheld, rapid fluorescence imaging system. Freshly processed eviscerated broiler carcasses (8-10 lb live weight), both normal (n=200) and septox (n=195), were collected from a local commercial poultry processor. Broiler carcasses were photographed using a handheld fluorescence spectral imaging system called the CSI-D+, a RGB camera with UV camera for fluorescence. The spectral camera and carcasses were placed in a box with a shackle attachment and images were taken. Normal broiler and septox carcasses had two images captured for different fluorescence exposure times (175 and 350ms; 230 and 270 ms). Images were collected for further image analysis using Convolution Neural Network deep learning (CNN-DL) algorithms. Data augmentation techniques were used to improve the complexity of collected images using transformation techniques including resizing, horizontal and vertical flip with random rotation. CNN model was developed on Google Collaboratory platform using CUDA 11.2 and Pytorch machine learning framework with 3 ConvNet layers. Adam Optimizer (learning rate =0.001, weight decay = 0.0001) with cross entropy loss function was used for training of model with 50 epoch. Septox and normal images were differentiated with a 98% accuracy with the testing model and 100% accuracy with the validation model. Results indicate that the CSI-D+ imaging system can provide image data to eliminate error in sorting septox affected broiler carcasses through fluorescent imaging.

Along with sep-tox being identified through spectral imaging, fecal contamination can be observed using the CSI-D+ camera, which has a zero-tolerance policy in the poultry processing industry enforced by the USDA-FSIS to prevent the spread of foodborne pathogens to consumers. The objective for this study was to assist in the identification of fecal matter on

processed chicken carcasses that cannot be seen with the human naked eye using a fluorescence imaging system through still images. A total of fifty chicken carcasses were collected from a processing plant. Four different types of fecal contamination (digesta, small intestine, large intestine, and ceca) were used to place on the breast of whole-chicken carcasses for comparison. Chicken carcasses were placed in an ambient light-free box and observed with a spectral handheld imaging system. Visually, the spectral images exhibited a red color in the area contaminated with fecal matter. Developed CNN-DL algorithm was able to identify the fecal matter presence on the chicken carcasses. Fecal matter present on the chicken carcasses was able to be identified by the spectral camera. Image analysis was performed through deep learning algorithms to classify broiler carcasses with fecal matter to determine which carcasses should be reprocessed for the establishment of food safety standards for future processing line automated imaging on carcass condemnations. Spectral imaging system can be deployed in poultry processing plants to detect fecal contamination and ultimately improve food safety. The significance of this study is for the identification of condemnations done to the carcass through a spectral imaging system to prevent foodborne illness and the implementation of food safety standards.

Research was conducted to evaluate a spectral imaging technology to detect visible fecal matter to improve automation in processing plants. Further, we investigated if the imaging system could detect fecal contamination after the WOGs are reworked (washed) and that invisible (to human eye) fecal can be a source of *Salmonella* contamination. Processed eviscerated broiler carcasses (8-10lbs live weight) were collected in a processing plant. Fecal contamination from the ceca (~100g) was collected and inoculated with an 18h *Salmonella* Typhimurium culture which was then placed on the breast skin of the chicken

carcass for examination. Inoculated carcasses (n=100) were hung by shackle in an ambient light-free box and imaged with a handheld spectral imaging system. Images were taken before inoculation, after inoculation, and after spraying the fecal contaminated area of carcasses with water. Images taken were used for further image analysis using Microsoft Custom Vision. Carcasses were swabbed after each taken image and incubated for 24 hours in Brain Heart Infusion (BHI) broth for BioMerieux GeneUp *Salmonella* PCR assay testing. Images determined that fecal contamination can be detected using the spectral camera. Moreover, the image analysis indicated that the remnants of fecal contamination, invisible to human eye, were present on the WOGs. *Salmonella* analysis of all 100 WOGs pre-fecal contamination were negative for the pathogen while those spots were found to be positive for *Salmonella* after reworking the carcasses to remove fecal matter. Custom Vision classification results had 100% precision and 83.3% recall concluding to have a 99.4% accuracy percentage. The research indicates a need to improve reworking and developing improved protocols for removing all traces of fecal contamination to improve food safety.